

Deeply Virtual Meson Production with CLAS

Valery Kubarovsky
Jefferson Lab



May 18-21, 2010
Thomas Jefferson National Accelerator Facility
Newport News, Virginia USA

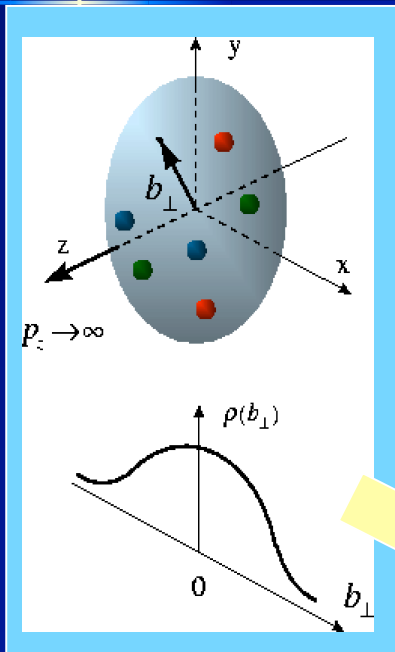
Outline

- Introduction
- DVMP theoretical models
- π^0/η electroproduction
 - Cross sections
 - Structure functions
 - Beam spin asymmetry
 - Cross sections ratio
- Summary

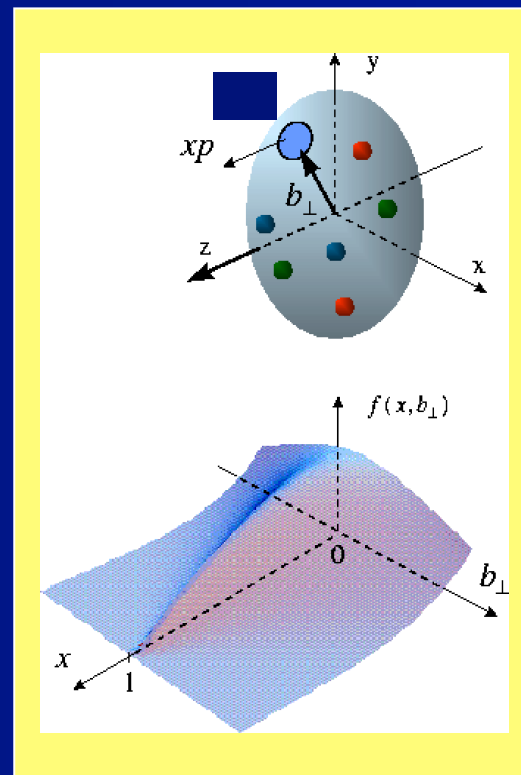
How are the proton's charge densities related to its quark momentum distribution?

D. Mueller, X. Ji, A. Radyushkin, ... 1994 -1997

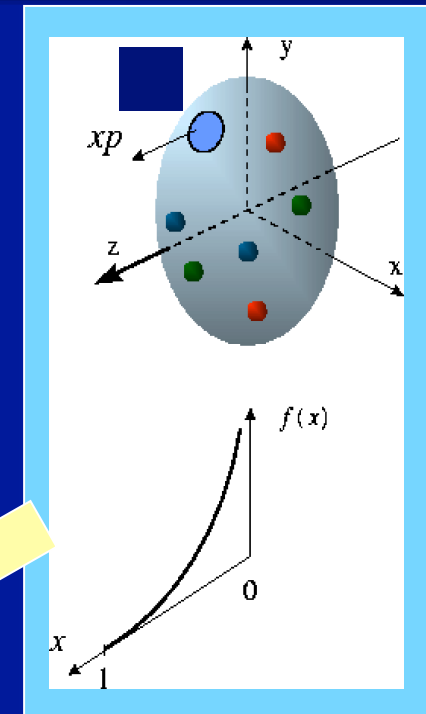
M. Burkardt, A. Belitsky... Interpretation in impact parameter space



Proton form factors,
transverse charge &
current densities



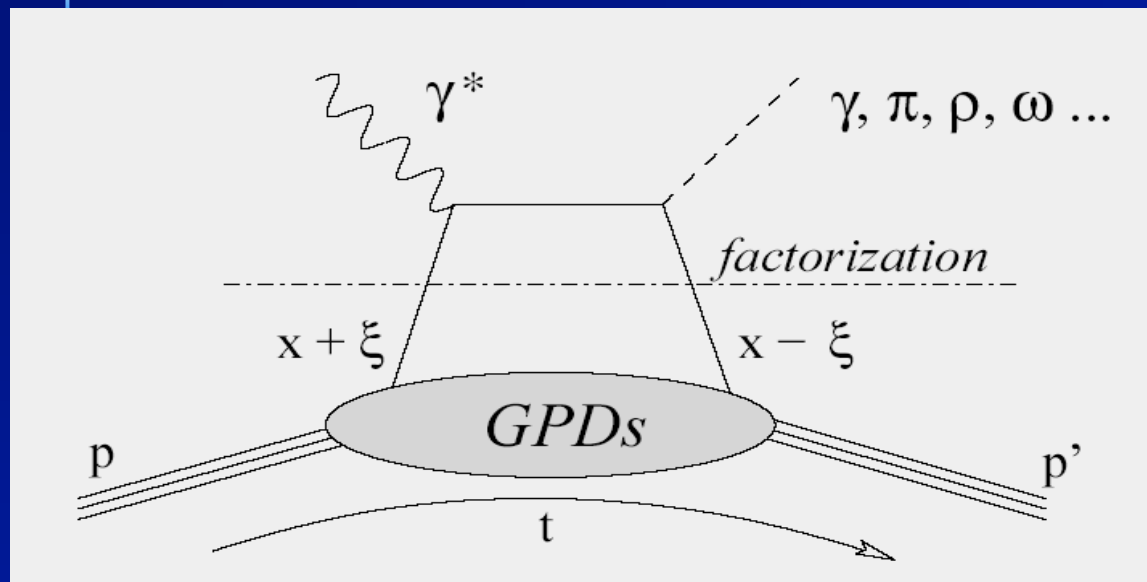
Correlated quark momentum
and helicity distributions in
transverse space - **GPDs**



Structure functions,
quark **longitudinal**
momentum & spin
distributions

Basic Process – Handbag Mechanism

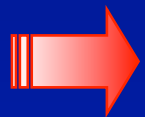
Deeply Virtual Compton Scattering (DVCS)
Deeply Virtual Meson Production (DVMP)



x - longitudinal quark momentum fraction

2ξ - longitudinal momentum transfer

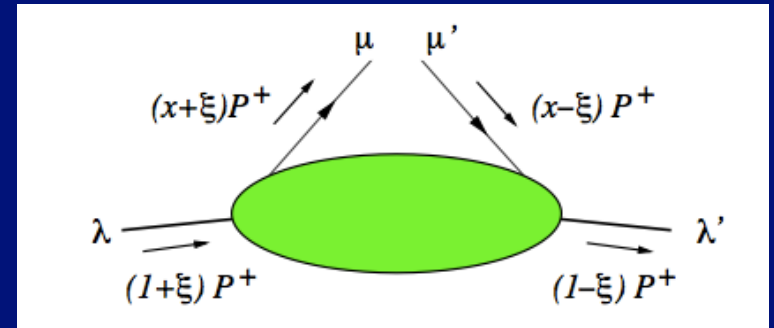
$\sqrt{-t}$ - Fourier conjugate to transverse impact parameter



GPDs depend on 3 variables, e.g. $H(x, \xi, t)$. They probe the quark structure at the amplitude level.

$$\omega = \frac{x_B}{2-x_B}$$

Generalized Parton Distributions



- There are 4 GPDs where partons do not transfer helicity $H, \tilde{H}, E, \tilde{E}$
- H and E are “unpolarized” and \tilde{H} and \tilde{E} are “polarized” GPD. This refers to the parton spins.
- 4 GPDs flip the parton helicity $H_T, \tilde{H}_T, E_T, \tilde{E}_T$

Basic GPD properties

- Forward limit

$$\begin{aligned}H^q(x, 0, 0) &= q(x) \\ \tilde{H}^q(x, 0, 0) &= \Delta q(x) \\ H_T^q(x, 0, 0) &= h_1^q(x)\end{aligned}$$

- Form factors

$$\begin{aligned}\int_{-1}^1 dx H^q(x, \xi, t) &= F_1^q(t), & \int_{-1}^1 dx E^q(x, \xi, t) &= F_2^q(t) \\ \int_{-1}^1 dx \tilde{H}^q(x, \xi, t) &= g_A^q(t), & \int_{-1}^1 dx \tilde{E}^q(x, \xi, t) &= g_P^q(t),\end{aligned}$$

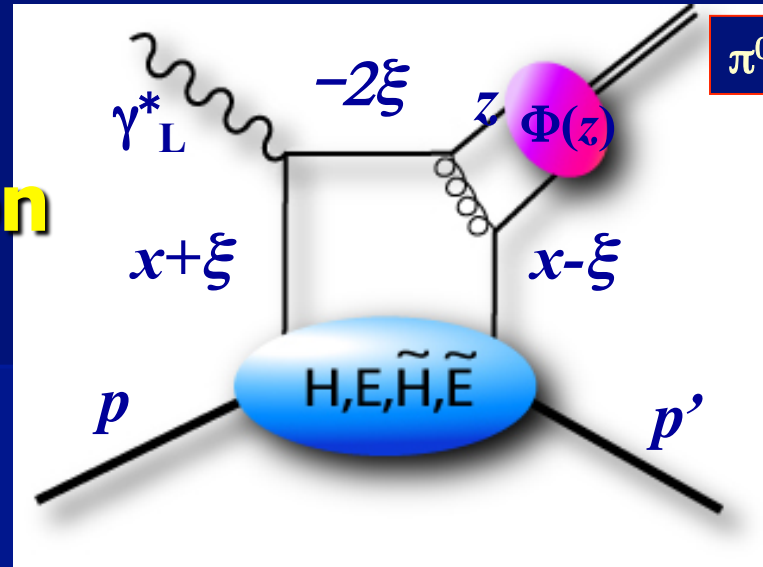
- Angular Momentum

$$J^q(t) = \frac{1}{2} \int_{-1}^1 dx x [H^q(x, \xi, t) + E^q(x, \xi, t)]$$

(Ji's sum rule)

High Q^2 , Low t Region

Collins, Frankfurt, Strikman - 1997



$\pi^0, \eta, \rho^0, \omega, \phi \dots$

- Factorization theorem states that in the limit $Q^2 \rightarrow \infty$ exclusive electroproduction of mesons is described by hard rescattering amplitude, generalized parton distributions (GPDs), and the distribution amplitude $\Phi(z)$ of the outgoing meson.
- The prove applies only to the case when the virtual photon has **longitudinal polarization**
- $Q^2 \rightarrow \infty$ $\sigma_L \sim 1/Q^6$, $\sigma_T/\sigma_L \sim 1/Q^2$
- The full realization of this program is one of the major objectives of the 12 GeV upgrade

+ t.c.

Flavor Separation and Helicity-Dependent GPDs

- DVCS is the cleanest way of accessing GPDs. However, it is difficult to perform a **flavor separation**.
- Vector and pseudoscalar meson production allows one to separate flavor and isolate the **helicity-dependent GPDs**.

Meson	GPD flavor composition
π^+	$\Delta u - \Delta d$
π^0	$2\Delta u + \Delta d$
η	$2\Delta u - \Delta d$
ρ^0	$2u + d$
ρ^+	$u - d$
ω	$2u - d$

$$\tilde{H}, \tilde{E}$$

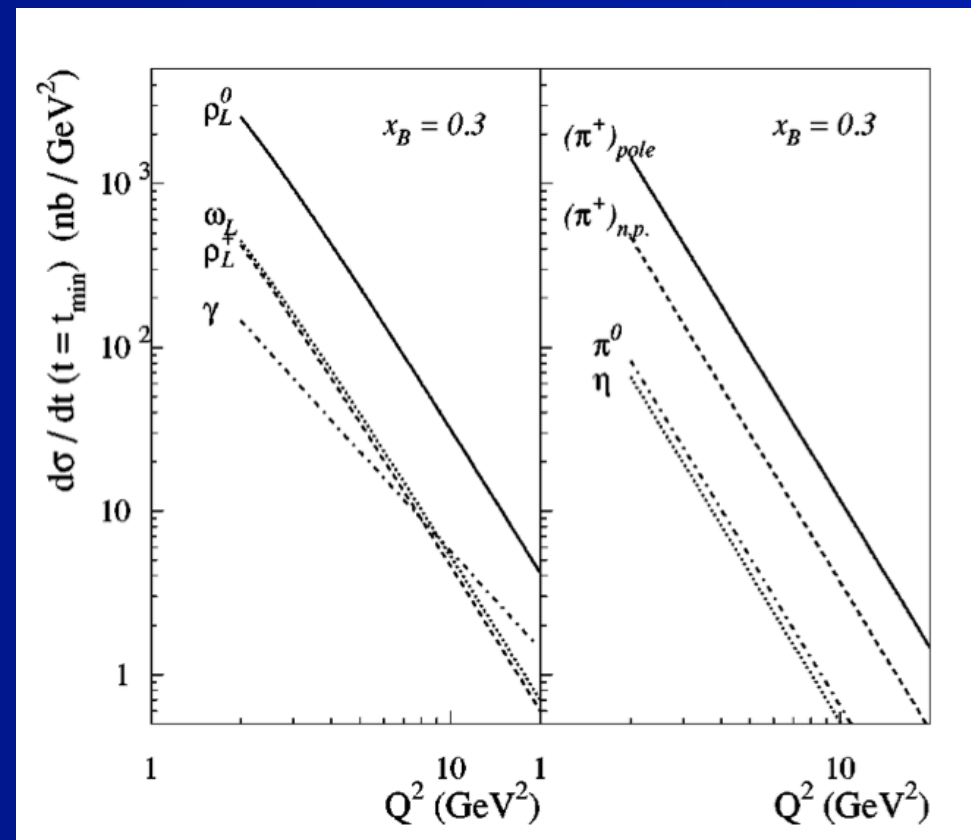
$$H, E$$

GPD predictions (only σ_L)

Vanderhaeghen, Guichon, Guidal, 1999

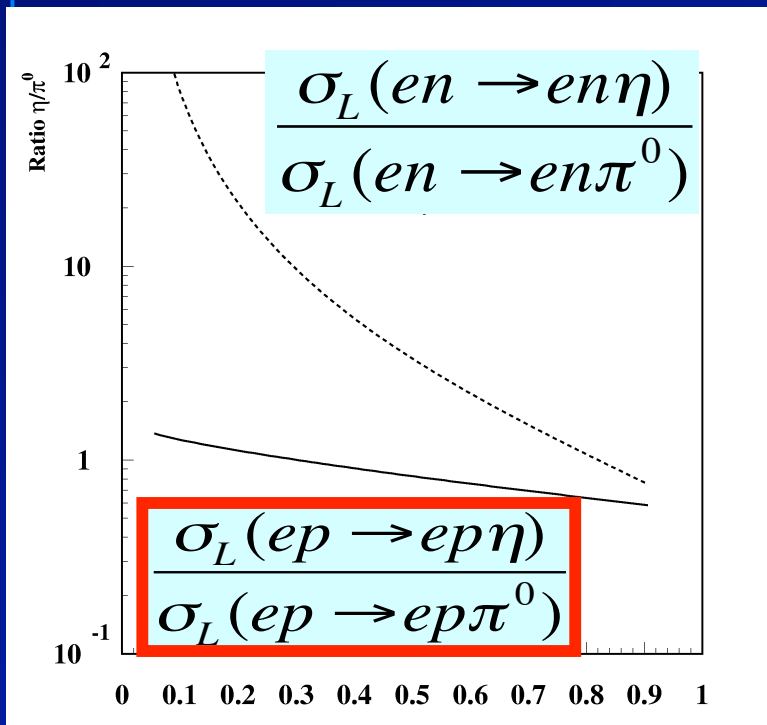
$$\frac{d\sigma_L}{dt} (t = t_{\min})$$

- $d\sigma_L/dt(t=t_{\min})$ for vector mesons (left panel)
- Pseudoscalar mesons (right panel)
- Note the pion pole contribution to the π^+ electroproduction (shown separately)

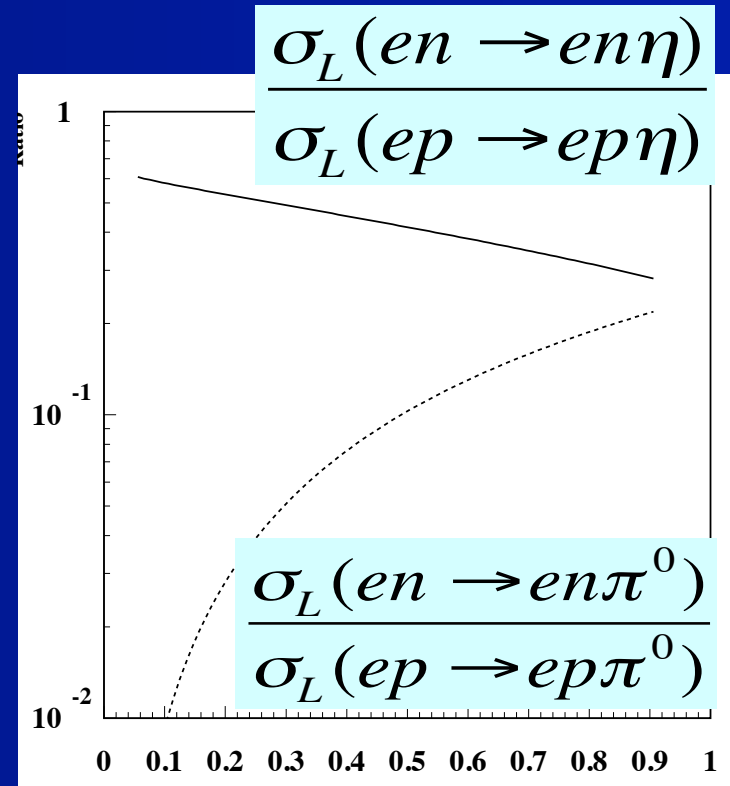


Cross Section Ratios as a function of x_B

Eides, Frankfurt, Strikman -1997



x_B



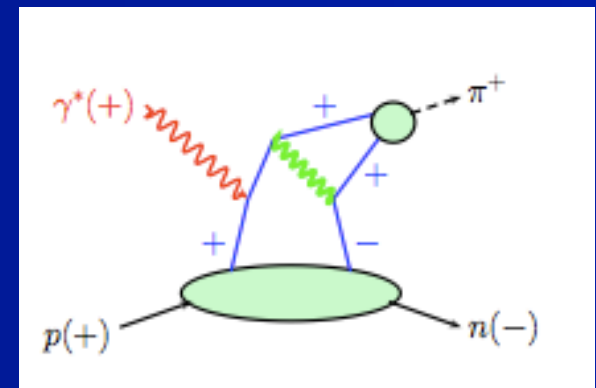
x_B

Transversity in DVMP

Kroll, Goloskokov
Goldstein, Luiti

- The data clearly show that a leading-twist calculation of DVMP within the handbag is insufficient. They demand higher-twist and/or power corrections.
- There is a large contribution from the helicity amplitude $M_{0-,++}$. Such contribution is generated by the the helicity-flip or transversity GPDs in combination with a twist-3 pion wave function.
- This explanation established an interesting connection to transversity parton distributions. The forward limit of H_T is the transversity distribution.

$$M_{0-,++} \sim H_T$$



$$H_T(x,0,0) = h_1(x)$$

π^0 electroproduction Handbag predictions

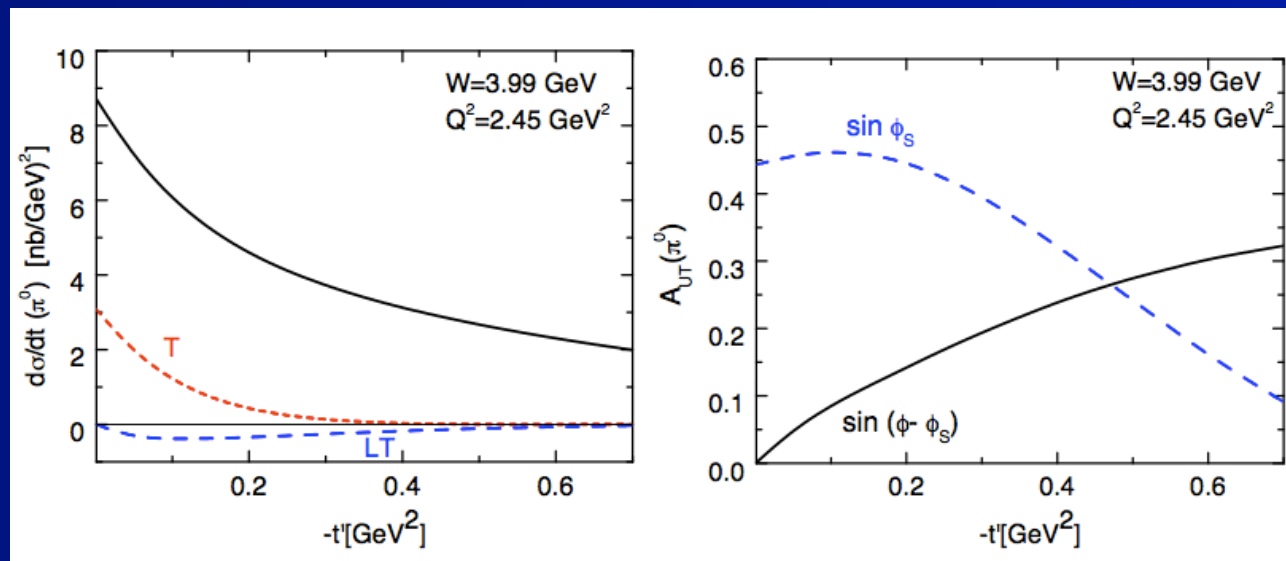


Kroll, Goloskokov, 2009.

$$\sigma_T + \epsilon \sigma_L$$

$$\sigma_T$$

$$\sigma_{LT}$$



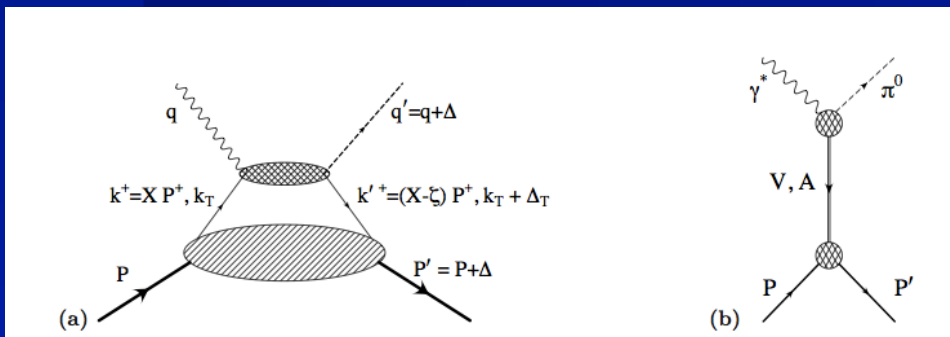
Predictions for the cross section (left) and A_{UT} (right) for the π^0 electroproduction versus $-t$. The unseparated (σ_L, σ_T) cross section was calculated as well as σ_T and σ_{LT} . At $W=2.2$ GeV the cross section will be a factor of 10 larger. We can check it at Jlab.

$$\gamma^* p \rightarrow p \pi^0$$

Nucleon Tensor Charge from Exclusive π^0 Electroproduction

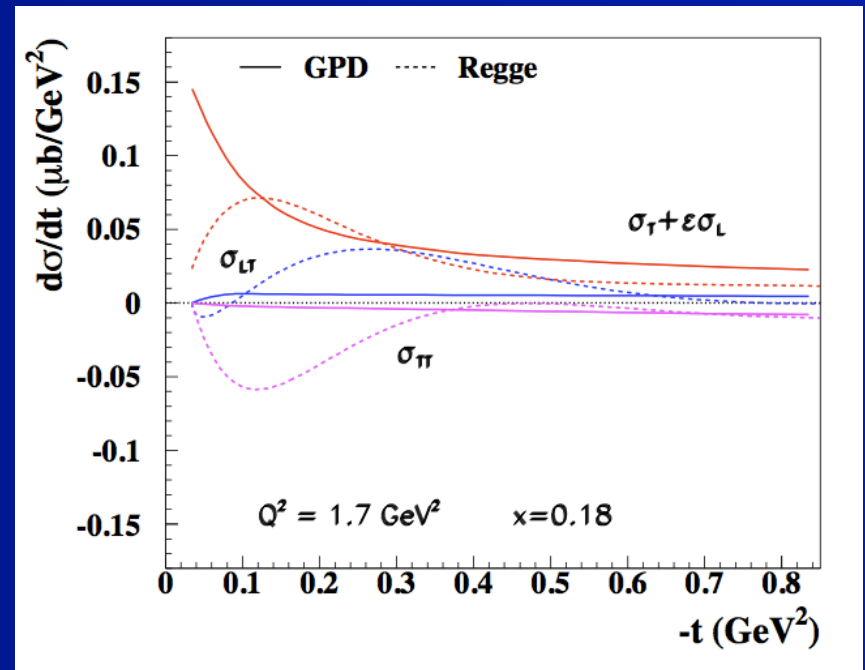
Ahmad, Goldstein, Luiti, 2009

- π^0 electroproduction proceeds through C-parity odd and chiral odd combination of t-channel exchange quantum numbers. This differs from DVCS and both vector and charge $\pi^{+/-}$ electroproduction, where the axial charge can enter the amplitudes.
- Contrary the tensor charge enters the π^0 process.



partonic degrees of freedom interpretation;

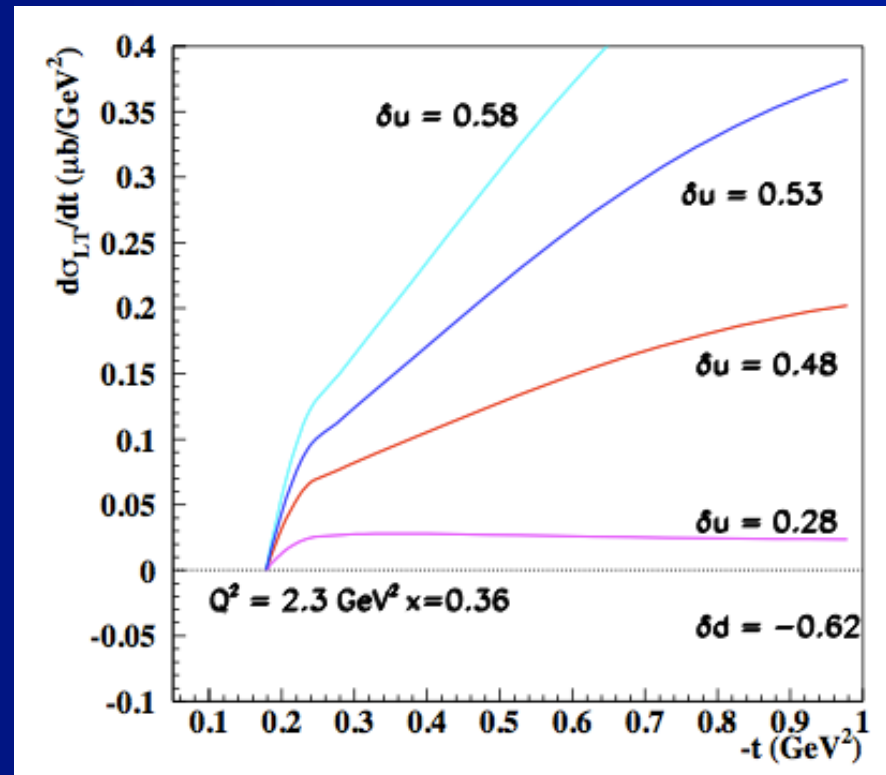
t-channel exchange diagram



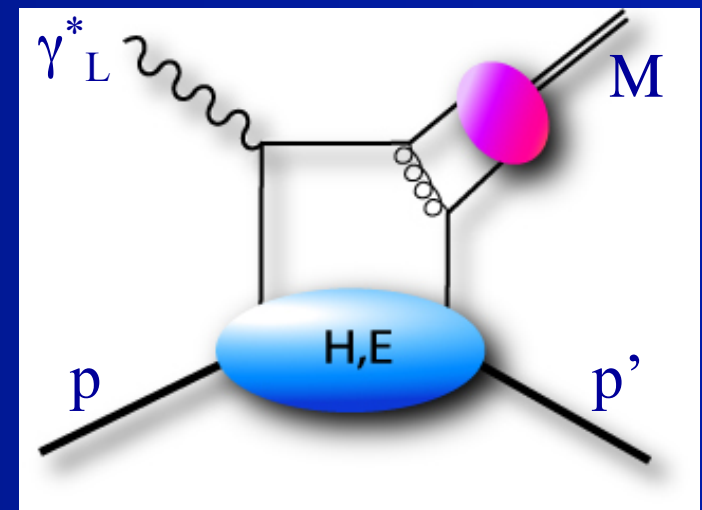
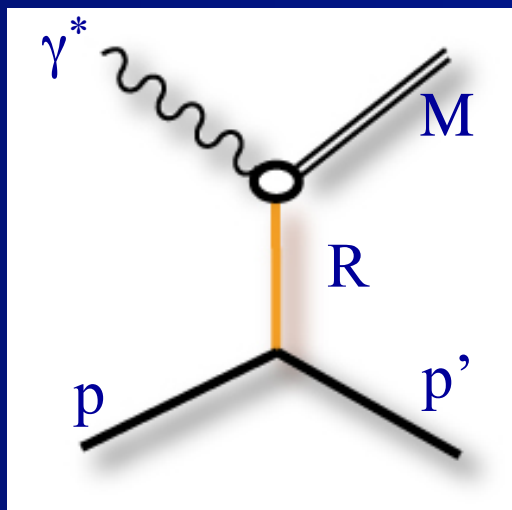
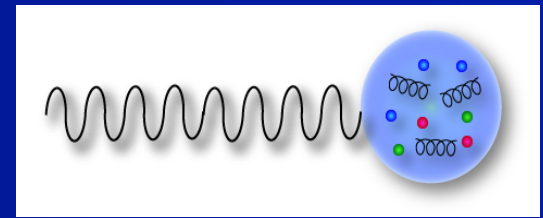
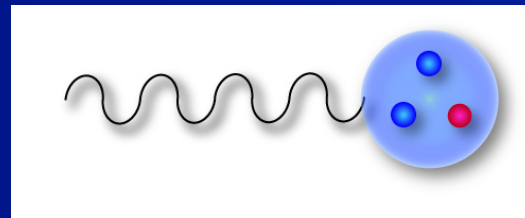
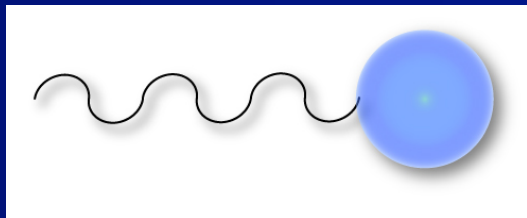
$$\gamma^* p \rightarrow p\pi^0$$

σ_{LT} for different values of the u quark tensor charge

Ahmad, Goldstein, Luiti, 2009



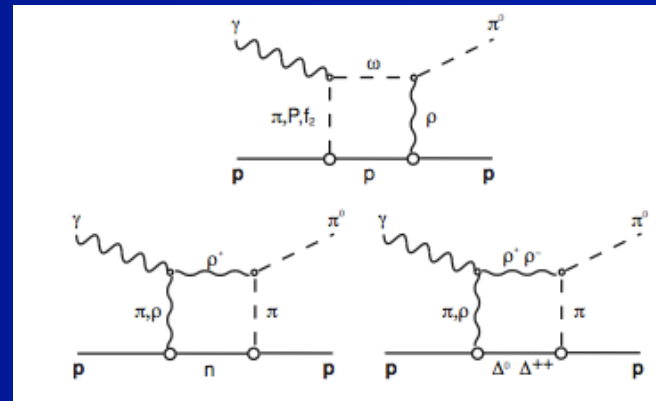
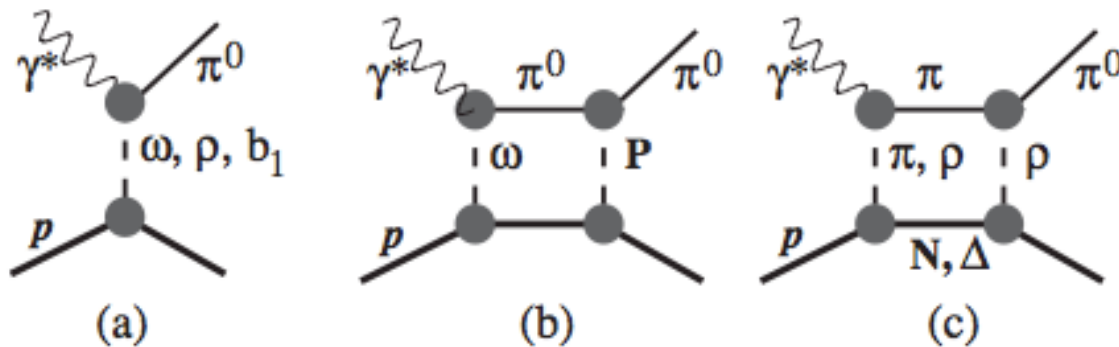
Transition from "hadronic" to the partonic degrees of freedom



$$\gamma^* p \rightarrow p \pi^0$$

Regge Model

J.M. Laget 2010



(a) Regge poles (vector and axial vector mesons)
 (b) and (c) pion cuts

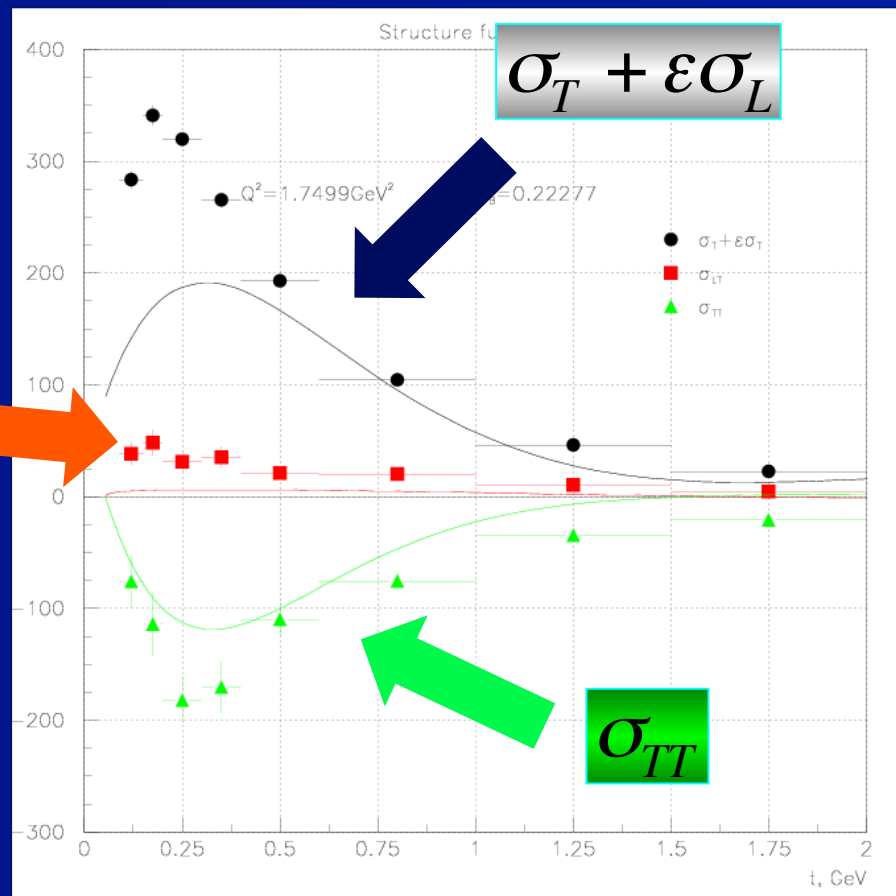
Vector meson cuts

$$\gamma^* p \rightarrow p\pi^0$$

Regge predictions

$Q^2=1.75$
 $x^B=0.22$

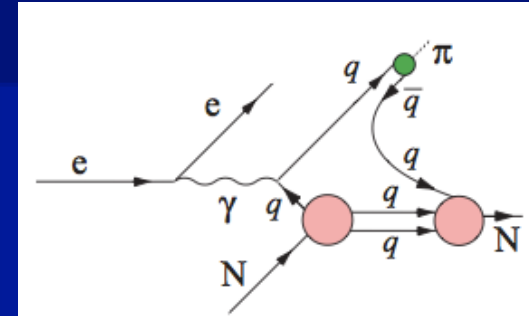
σ_{LT}



$-t, \text{GeV}^2$

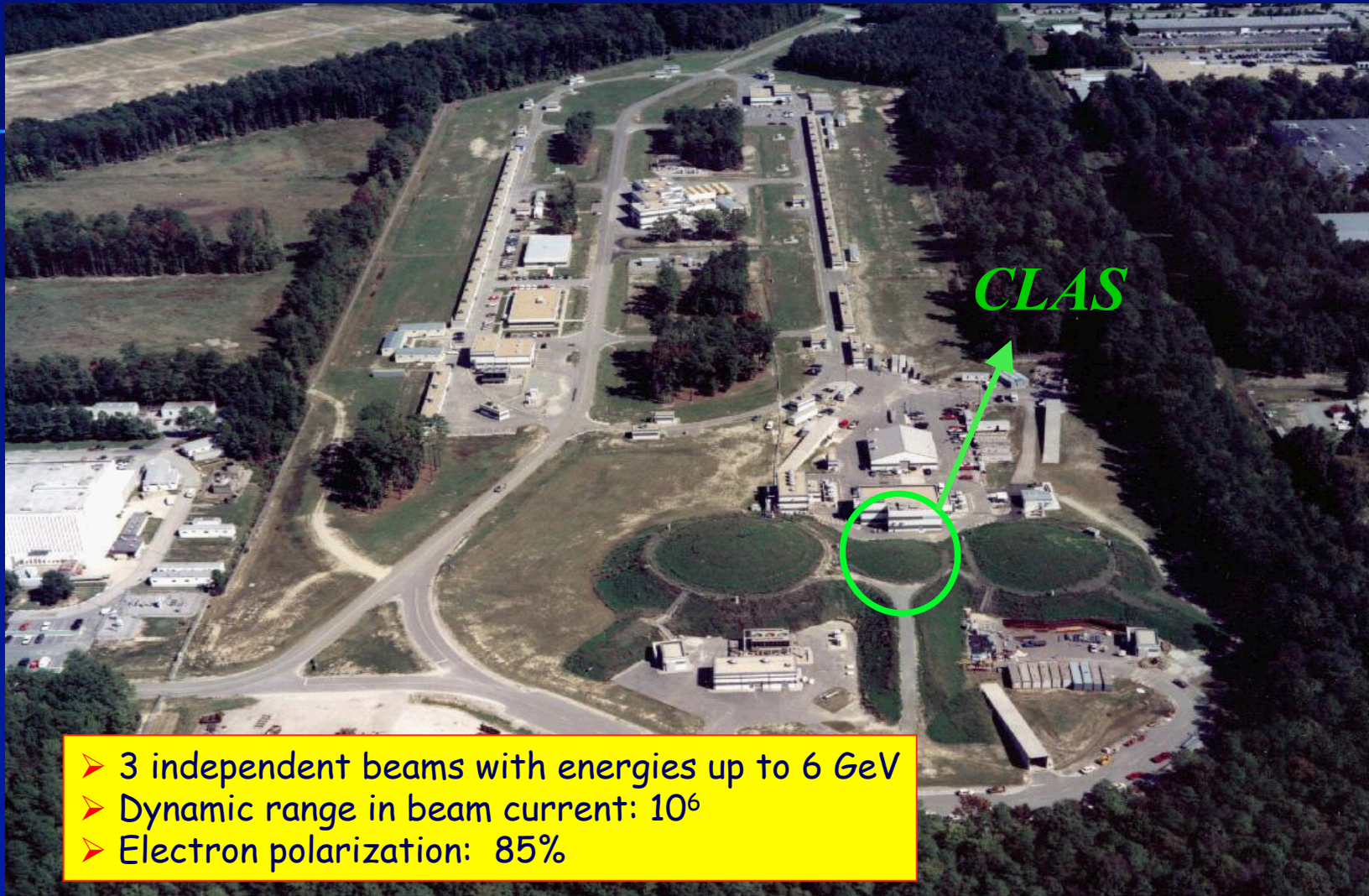
Combined Regge + DIS model

Kaskulov, Gallmeister, Mosel (2008-2010)



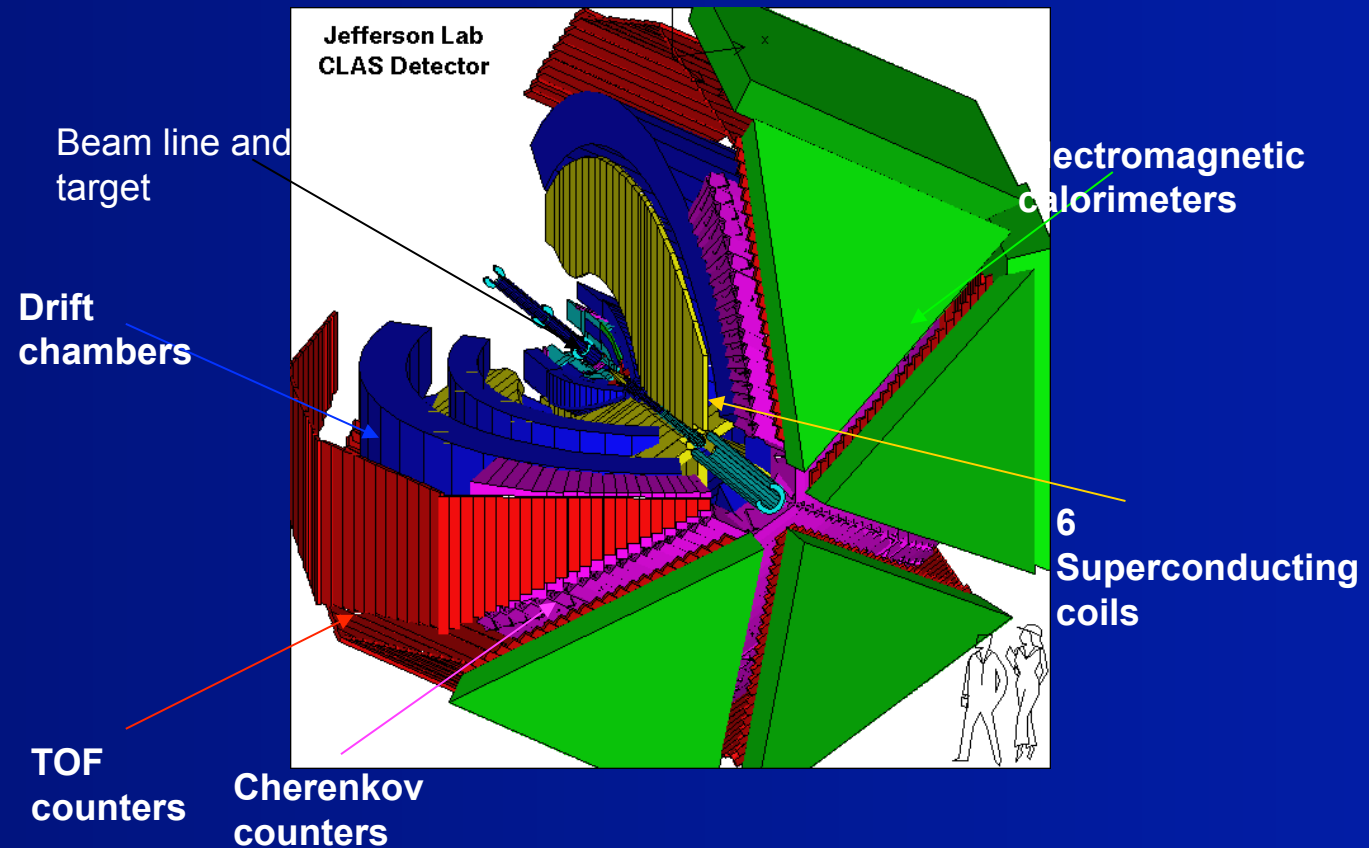
- σ_L is dominated by improved treatment of gauge Invariant Regge model.
- σ_T is described by direct hard interaction of virtual photons with partons followed by the hadronization process into πN channel.
- This explains the large transverse response at moderate and high photon virtualities.
- This process is sensitive to the intrinsic transverse momentum distribution of partons.

JLab Site: The 6 GeV Electron Accelerator



- 3 independent beams with energies up to 6 GeV
- Dynamic range in beam current: 10^6
- Electron polarization: 85%

CEBAF Large Acceptance Spectrometer CLAS



CLAS (forward carriage and side clamshells retracted)

Large angle EC

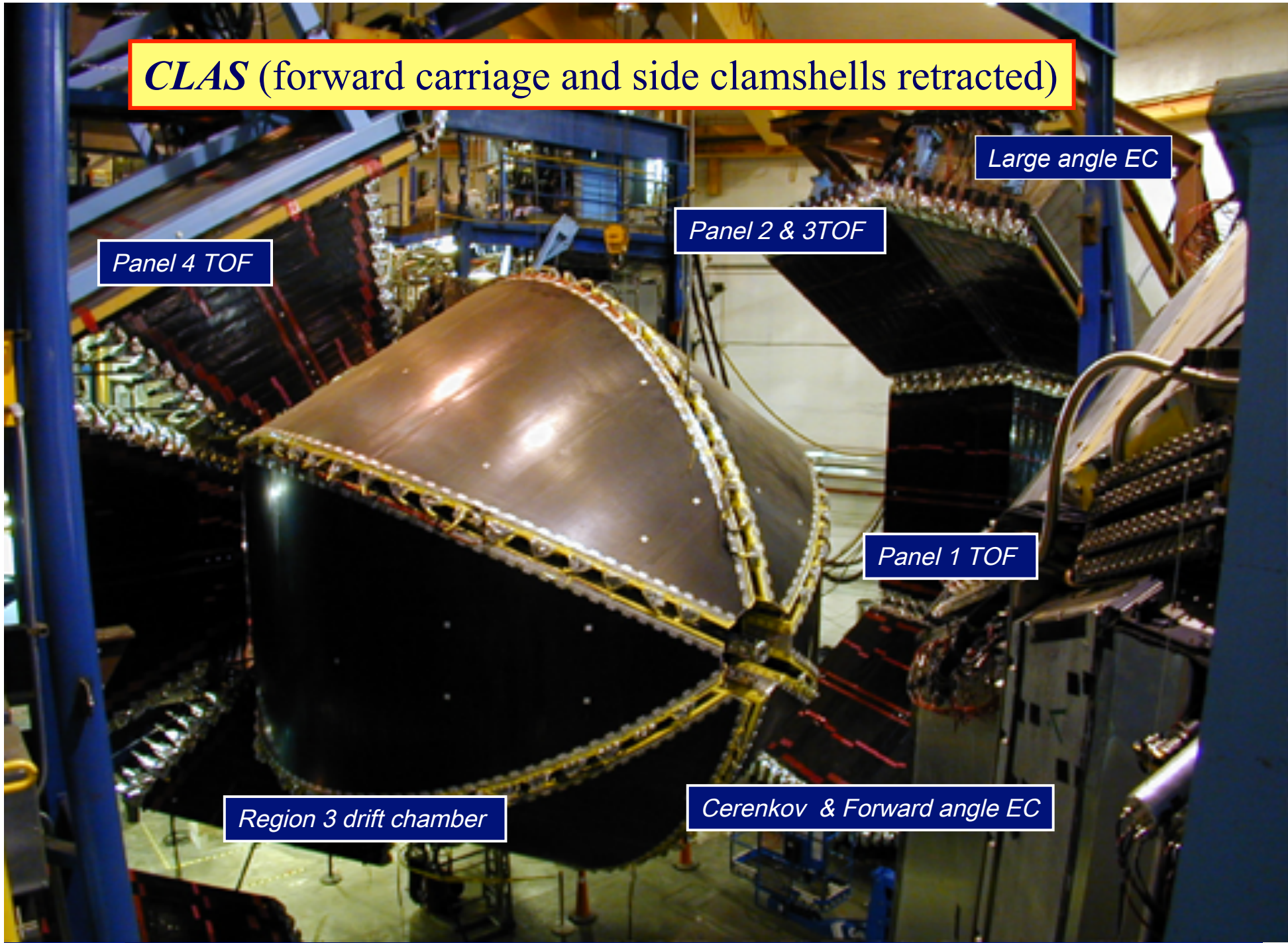
Panel 2 & 3 TOF

Panel 4 TOF

Panel 1 TOF

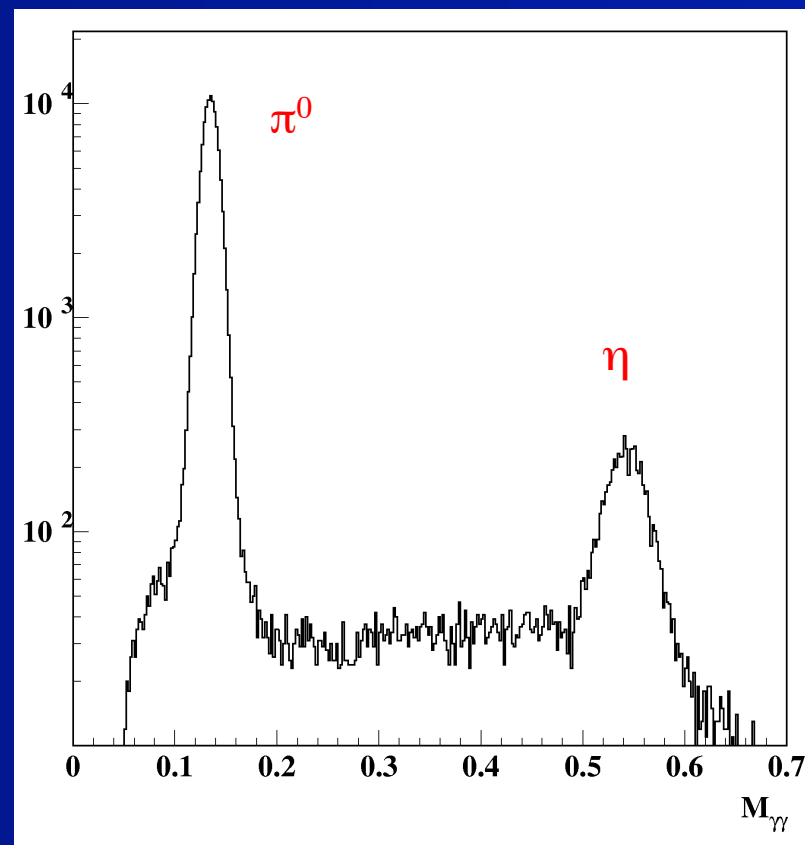
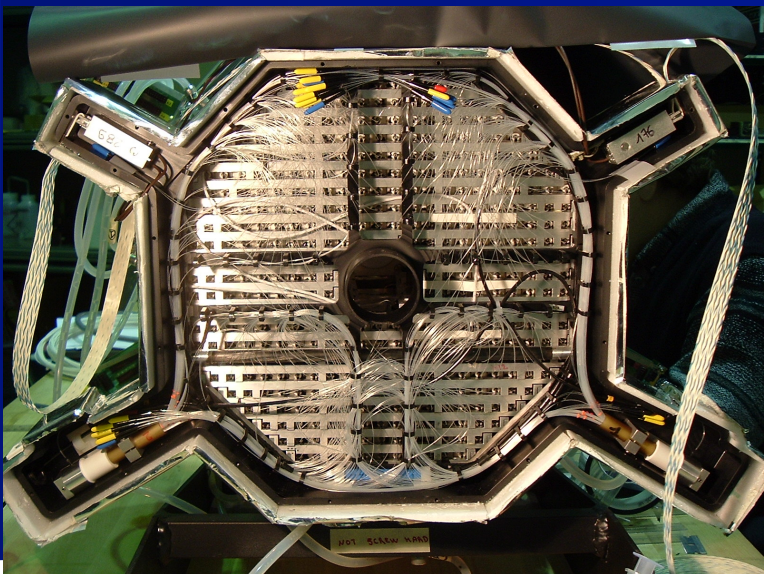
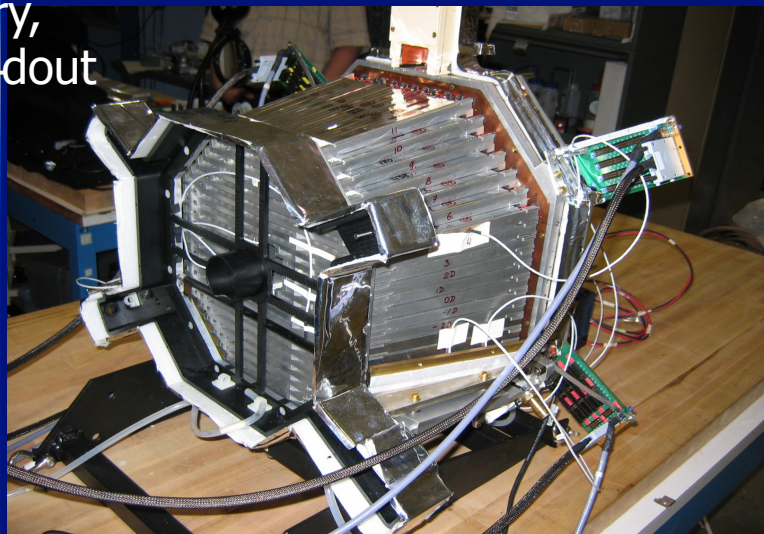
Region 3 drift chamber

Cerenkov & Forward angle EC



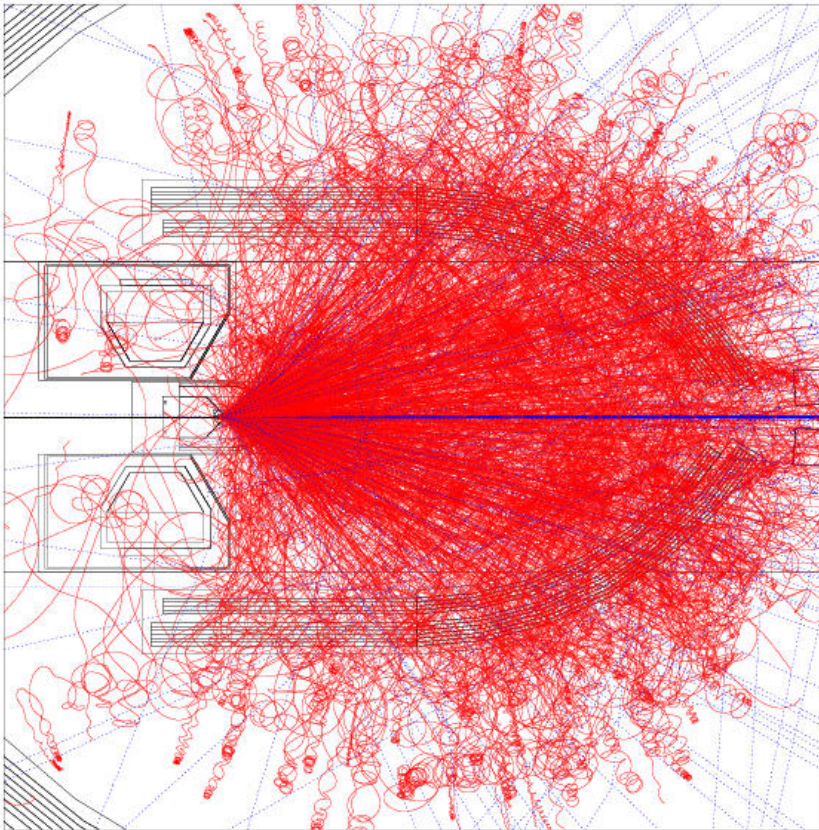
CLAS Lead Tungstate Electromagnetic Calorimeter

424 crystals,
18 RL,
pointing
geometry,
APD readout



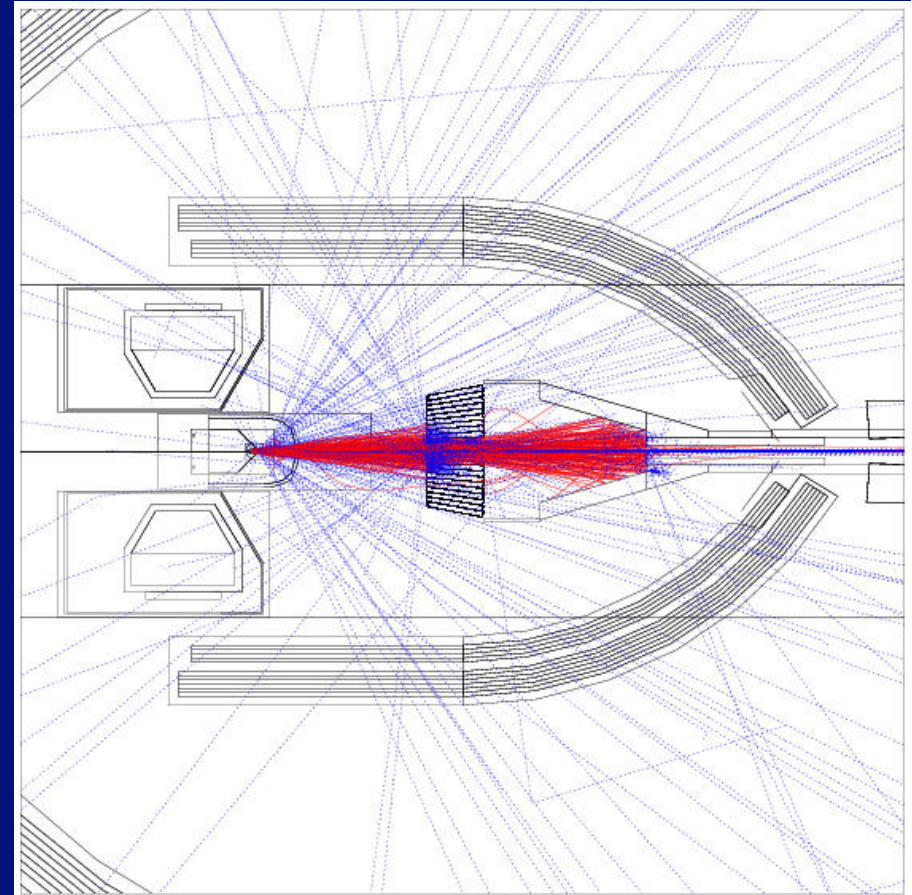
Møller electron shielding

Møller background **without** B field



Huge amounts of electrons drowning the tracking chambers in background.

Møller background **with** B field



Background electrons hitting the tracking chambers are eliminated.

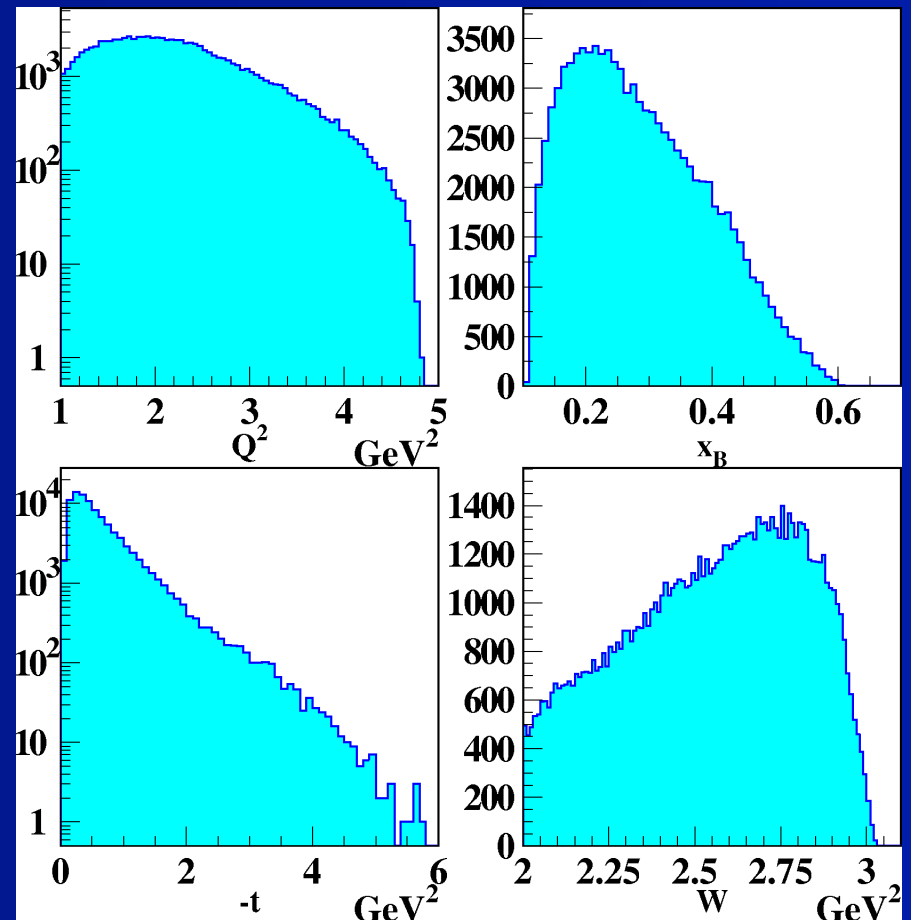
DVMP: Kinematic Coverage

4 dimensional grid in Q^2 , x_B , t , and ϕ

$$ep \rightarrow ep\pi^0, \quad \pi^0 \rightarrow \gamma\gamma$$

$$ep \rightarrow ep\eta, \quad \eta \rightarrow \gamma\gamma$$

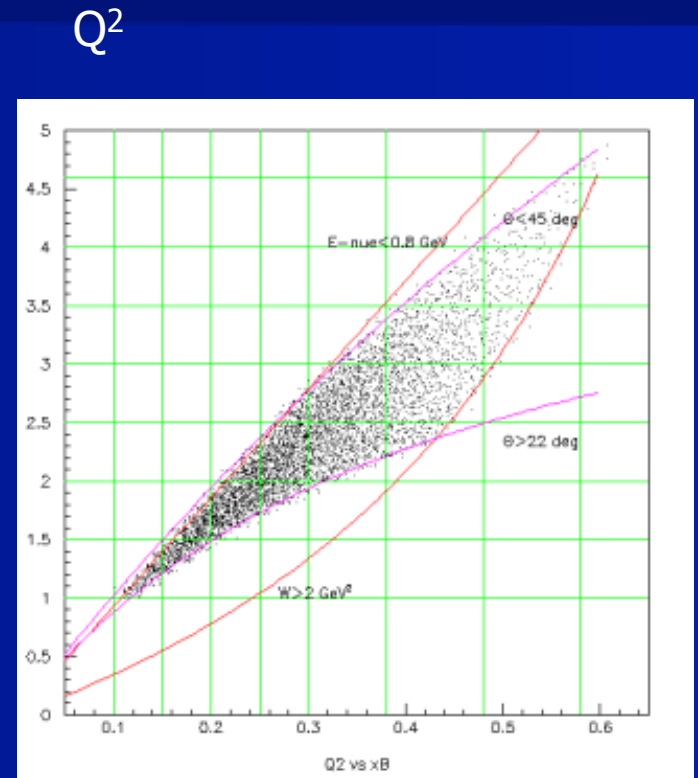
- Polarized Electron Beam
- $E_0 = 5.776$ GeV
- 75-80% polarization
- 2.5 cm Liquid Hydrogen target
- IC calorimeter
- Instant luminosity $2 \cdot 10^{34}$ cm²/s
- Integrated luminosity: $3.27 \cdot 10^7$ nb⁻¹



4 Dimensional Grid

Rectangular bins are used.

- Q^2 - 7 bins(1.-4.5 GeV^2)
- x_B - 7 bins(0.1-0.58)
- t - 8 bins(0.09-2.0 GeV)
- ϕ - 20 bins(0-360°)
- π^0 data \sim 2000 points
- η data \sim 1000 points



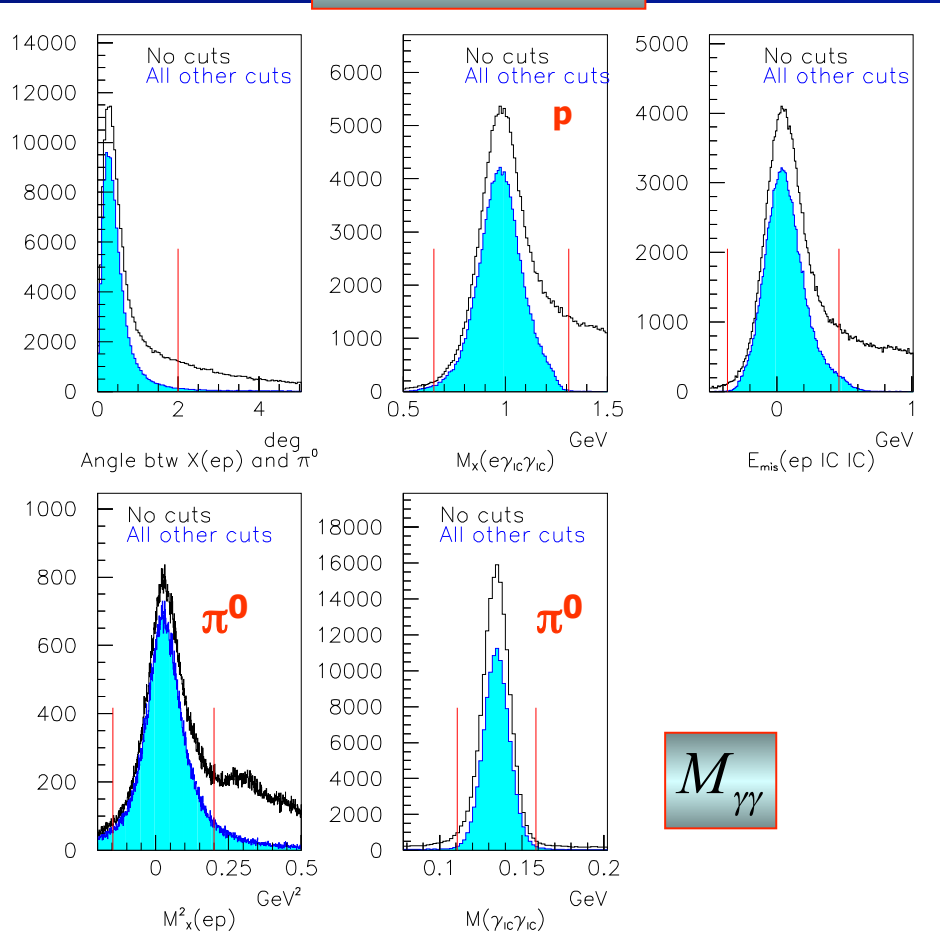
x_B

$$ep \rightarrow ep\pi^0, \quad \pi^0 \rightarrow \gamma\gamma$$

$$M_{\text{missing}}(e\gamma\gamma)$$

$$\theta(X_{\text{missing}}^{ep}, \gamma\gamma)$$

$$E_{\text{missing}}$$



$$M_{\text{missing}}^2(ep)$$

$$M_{\gamma\gamma}$$

$ep \rightarrow ep\eta, \eta \rightarrow \gamma\gamma$

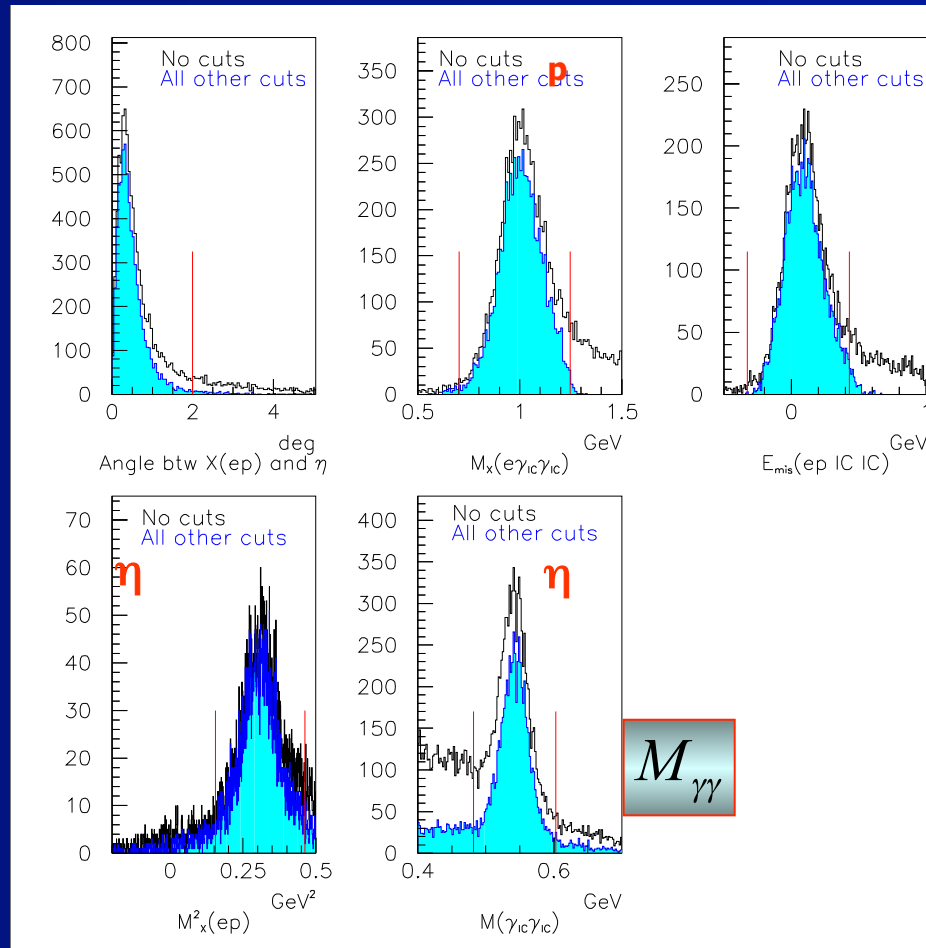
$$M_{\text{missing}}(e\gamma\gamma)$$

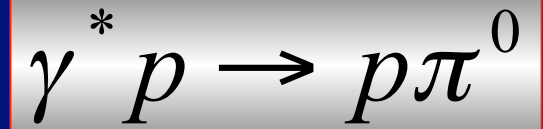
$$\theta(X_{\text{missing}}^{ep}, \gamma\gamma)$$

$$E_{\text{missing}}$$

$$M_{\text{missing}}^2(ep)$$

$$M_{\gamma\gamma}$$



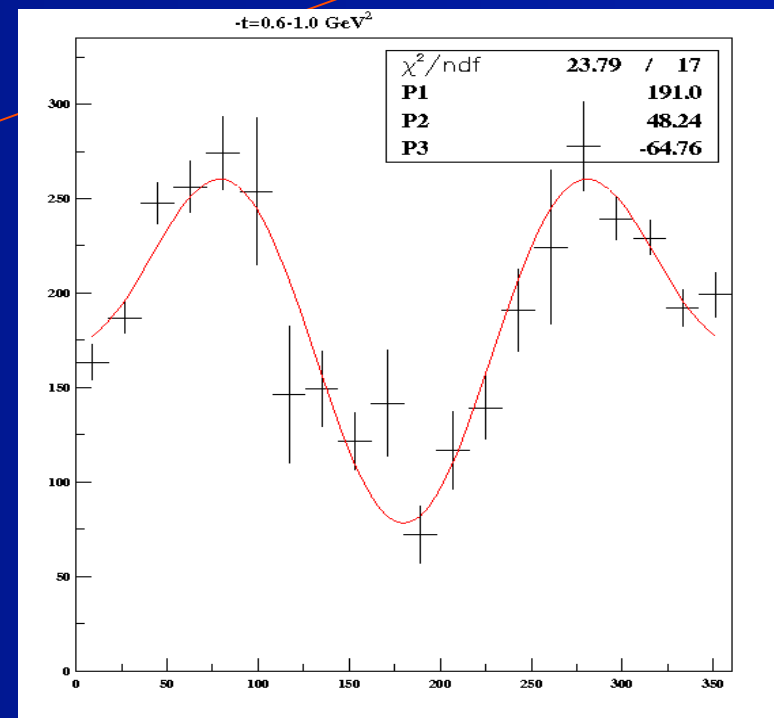


Structure Functions

$$\frac{d\sigma}{dt d\phi}(Q^2, x, t, \phi) = \frac{1}{2\pi} \left(\frac{d\sigma_T}{dt} + \varepsilon \frac{d\sigma_L}{dt} + \varepsilon \frac{d\sigma_{TT}}{dt} \cos 2\phi + \sqrt{2\varepsilon(\varepsilon + 1)} \frac{d\sigma_{LT}}{dt} \cos \phi \right)$$

Fit of the ϕ -distribution gives us three structure functions

$$\begin{aligned} & \frac{d\sigma_T}{dt} + \varepsilon \frac{d\sigma_L}{dt} \\ & \frac{d\sigma_{TT}}{dt} \\ & \frac{d\sigma_{LT}}{dt} \end{aligned}$$



Monte Carlo

- Empirical model for the structure cross sections was used for the MC simulation and radiative corrections
- This model is based on CLAS data
- MC simulation included the radiative effects and used empirical model for the Born term.
- 100 M events were simulated with GSIM program.

Cross section model

The package includes independent functions for the calculations of all structure functions: $\sigma_T, \sigma_L, \sigma_{TT}, \sigma_{LT}, \sigma_{LT}$.

The model is as follows:

- $\sigma_T = \sigma^T e^{B_T(x_B)t} / (Q^2 + M^2)^n, B_T(x_B) = \alpha^T * 2 * 1.1 * \ln(x_B)$
- $\sigma_L = \sigma^L Q^2 e^{B_L(x_B)t} / (Q^2 + M^2)^n, B_L(x_B) = \alpha^L * 2 * 1.1 * \ln(x_B)$
- $\sigma_{TT} = \sigma^{TT} (t - t_{min}) e^{B_{TT}(x_B)t} / (Q^2 + M^2)^n, B_{TT}(x_B) = \alpha^{TT} * 2 * 1.1 * \ln(x_B)$
- $\sigma_{LT} = \sigma^{LT} \sqrt{t - t_{min}} e^{B_{LT}(x_B)t} / (Q^2 + M^2)^n, B_{LT}(x_B) = \alpha^{LT} * 2 * 1.1 * \ln(x_B)$
- $\sigma_{LT} = 0$

where $\sigma^T, \sigma^L, \sigma^{TT}, \sigma^{LT}, \alpha^T, \alpha^L, \alpha^{TT}, \alpha^{LT}, M^2, n$ are free parameters. Note the different t-dependence for

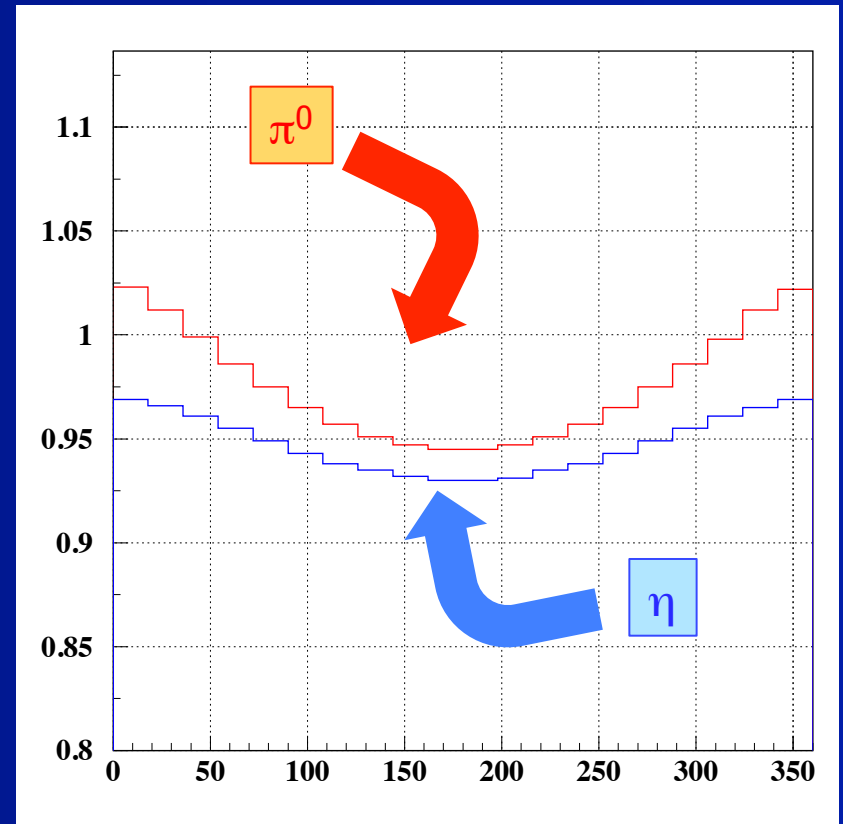
- $\sigma^{TT} \sim (t - t_{min})$ and
- $\sigma^{LT} \sim \sqrt{t - t_{min}}$.

Radiative Corrections

- Radiative Corrections were calculated using **Exclurad** package adapted by Kyungseon with structure cross sections described by our empirical cross section.

$$Q^2 = 1.15 \text{ GeV}^2 \quad x_B = 0.13 \quad -t = 0.1 \text{ GeV}^2$$

$$RadCor = \frac{\sigma_{Rad}}{\sigma_{Born}}$$



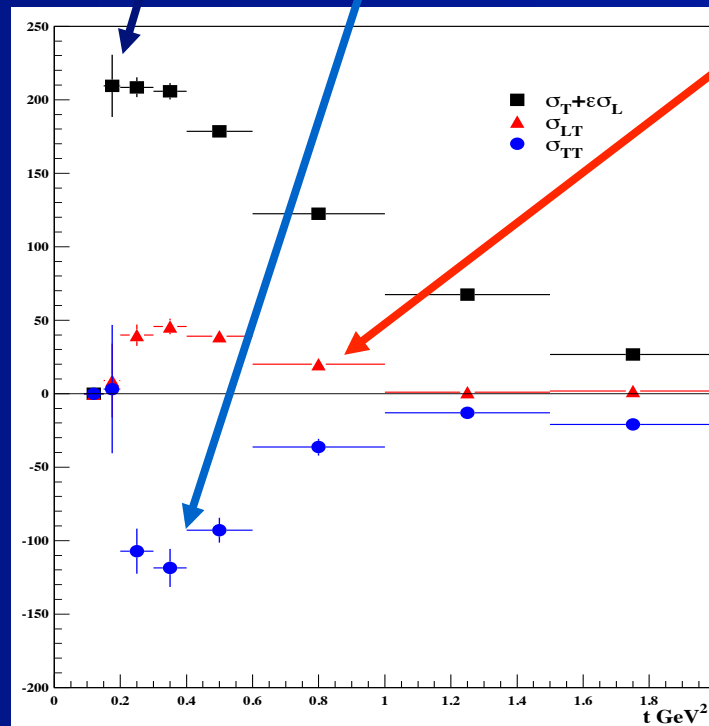
ϕ

$$\gamma^* p \rightarrow p\pi^0$$

$(\sigma_T + \varepsilon\sigma_L)$ σ_{TT} σ_{LT} as a function of t

$$\frac{d\sigma}{dt d\phi}(Q^2, x, t, \phi) = (\sigma_T + \varepsilon\sigma_L) + \varepsilon\sigma_{TT} \cos 2\phi + \sqrt{2\varepsilon(\varepsilon + 1)}\sigma_{LT} \cos \phi$$

Non-zero σ_{TT} and σ_{LT} imply that both transverse and longitudinal amplitudes participate in the process



$$Q^2 = 2.3$$

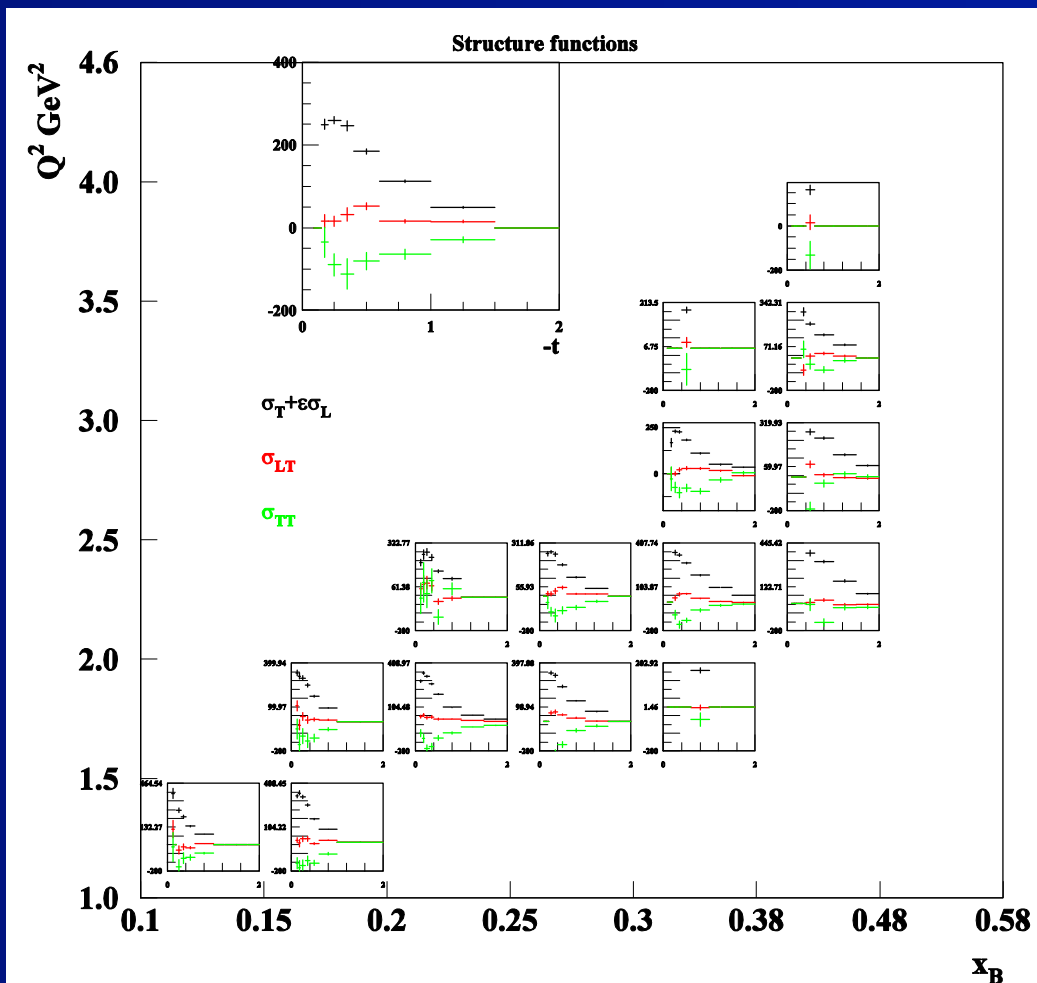
$$x_B = 0.4$$

t GeV²

Structure Functions

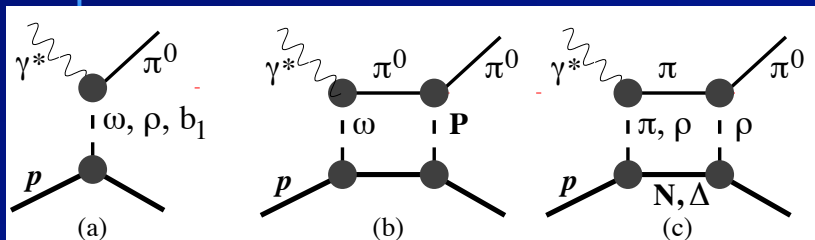
$$(\sigma_T + \varepsilon\sigma_L) \quad \sigma_{TT} \quad \sigma_{LT}$$

$$\gamma^* p \rightarrow p\pi^0$$



$$\gamma^* p \rightarrow p\pi^0$$

$(\sigma_T + \epsilon\sigma_L)$ σ_{TT} σ_{LT} in Regge Model (J-M Laget)

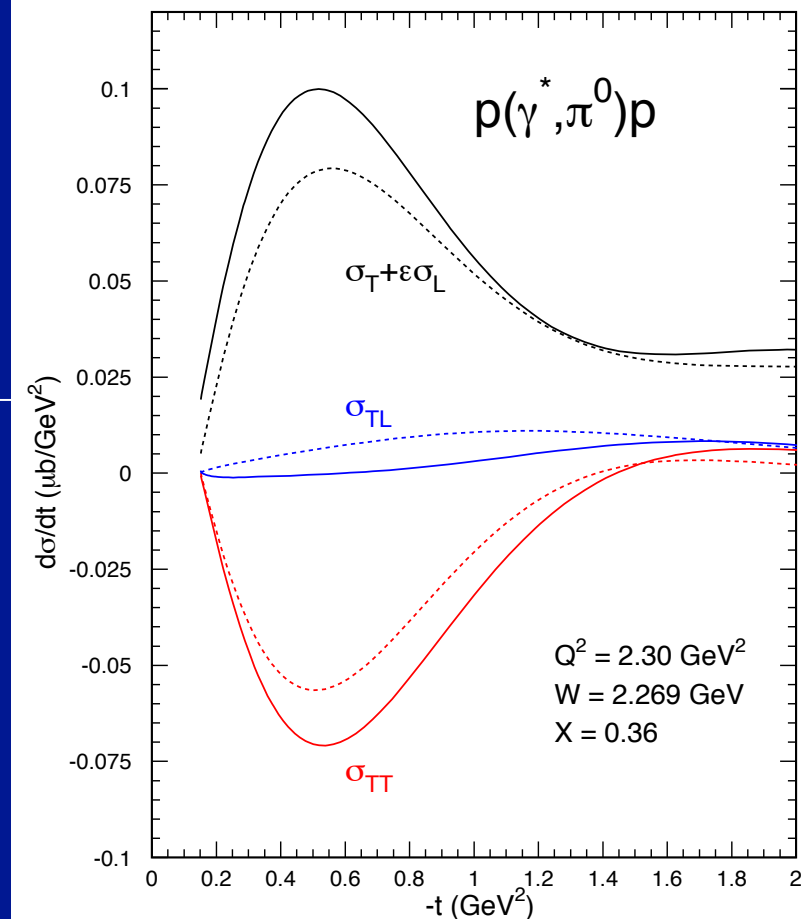


$\omega/\rho/b_1$

elastic rescat.

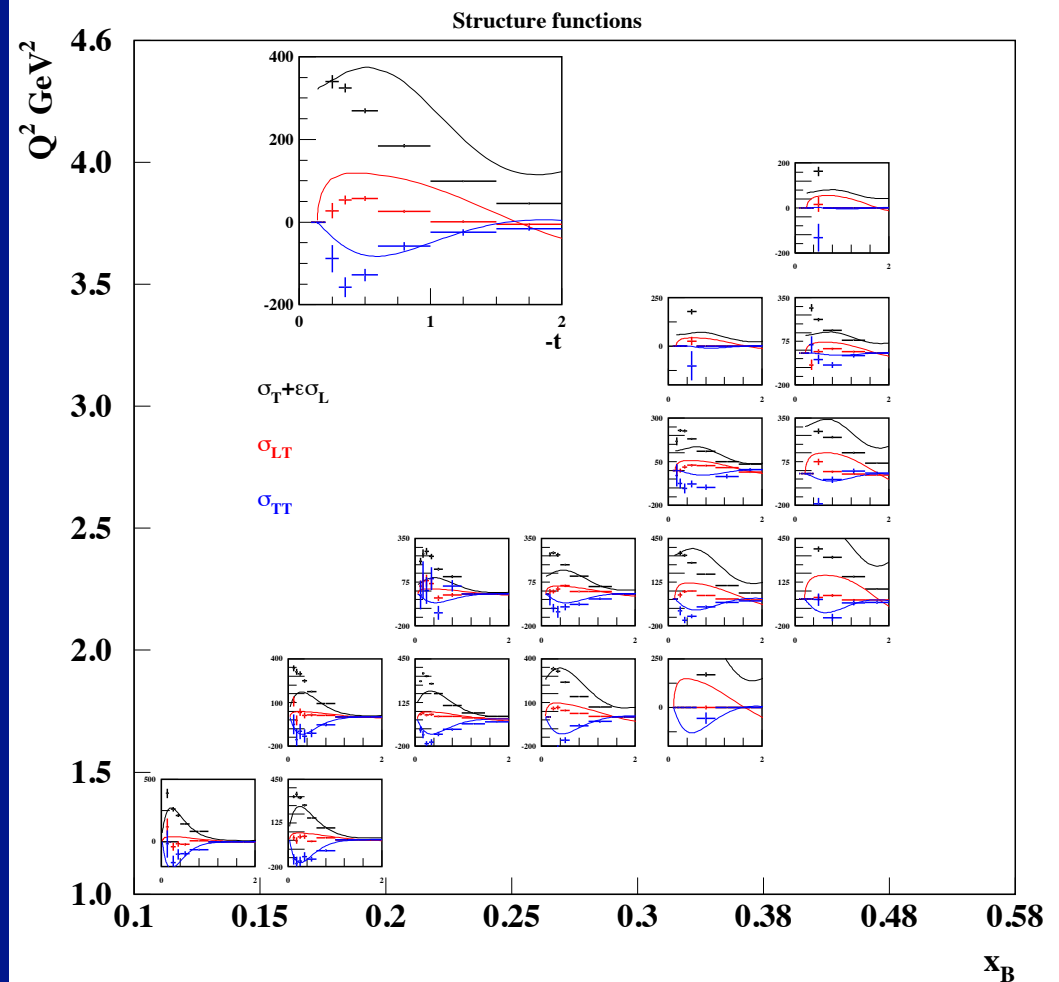
charge pion

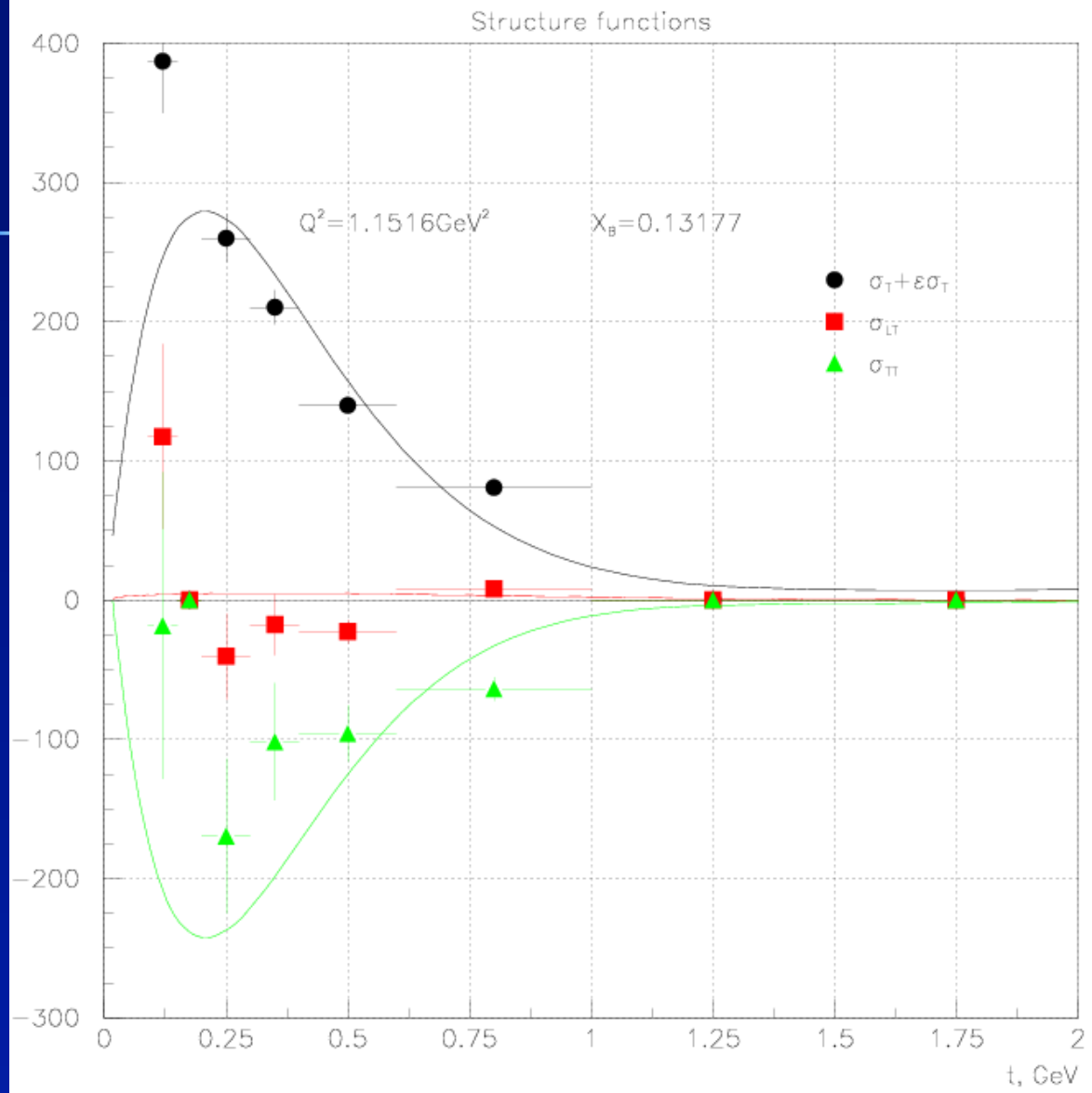
- The dashed lines correspond to the $\omega/\rho/b_1$ Regge poles and elastic rescattering
- The full lines include also charge pion nucleon and Delta intermediate states.
- Regge model qualitatively describes the experimental data



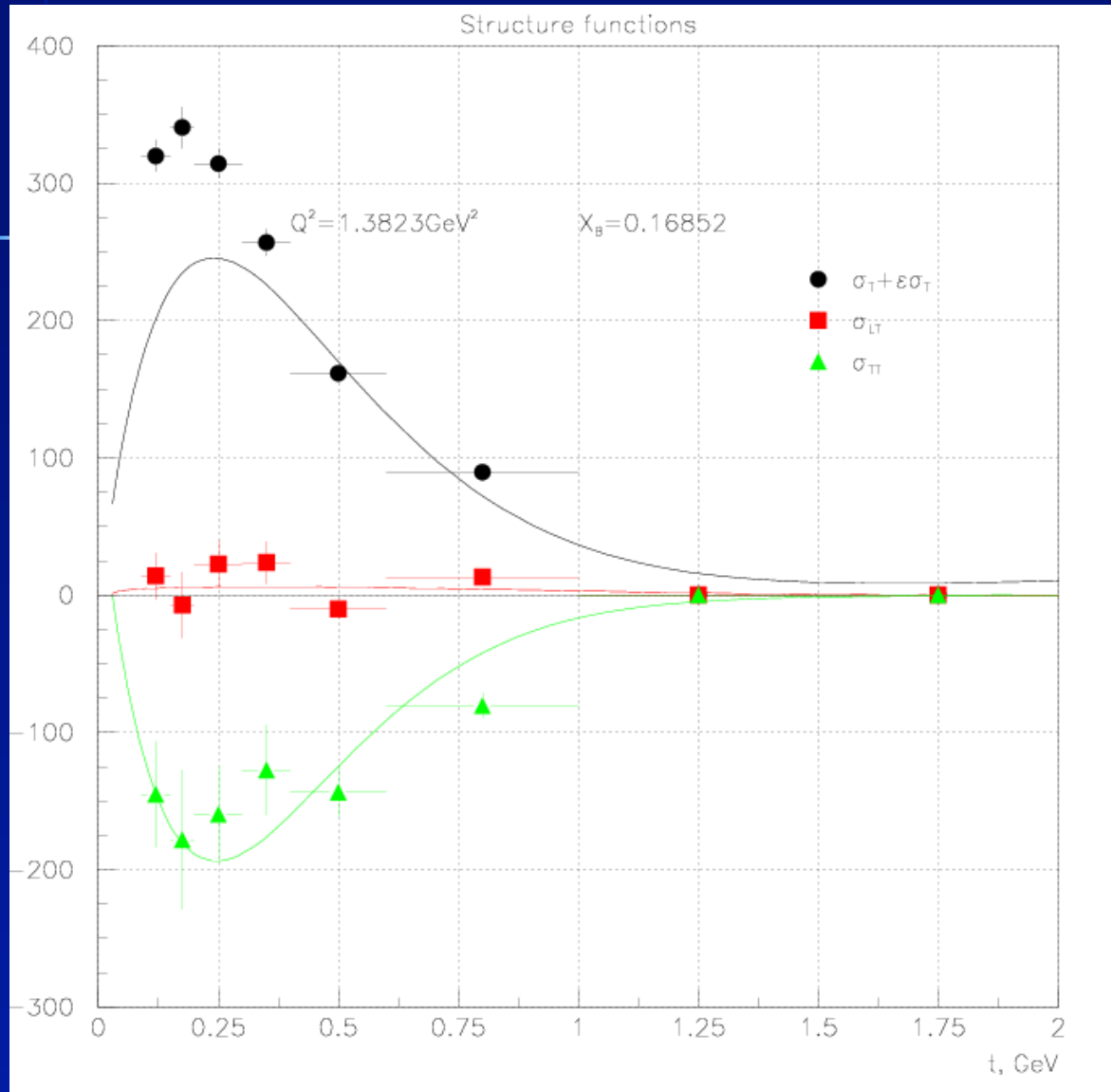
Comparison with J.M. Laget Regge model

- Extracted reduced cross sections were compared with predictions of J.M. Laget Regge Model

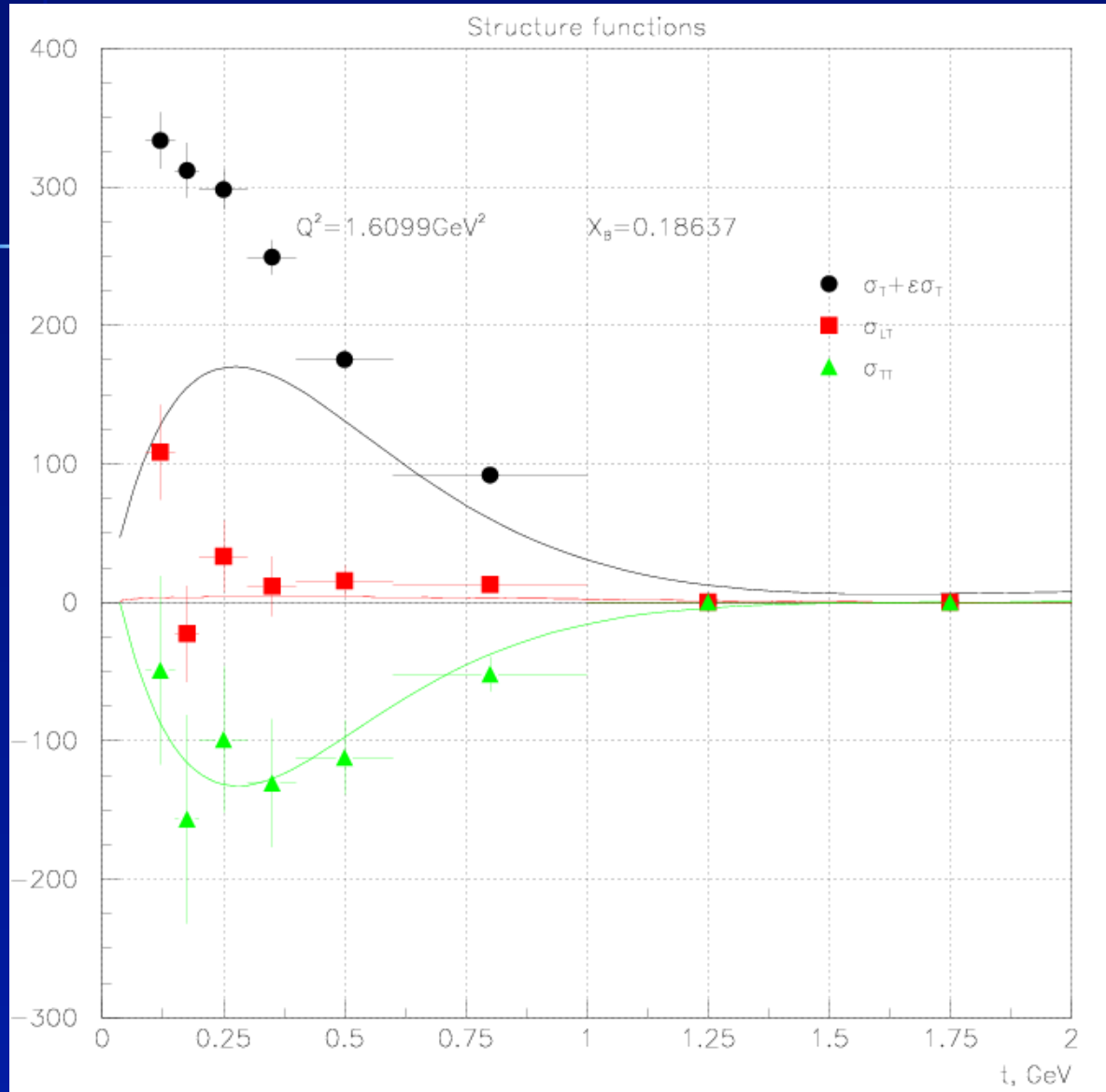




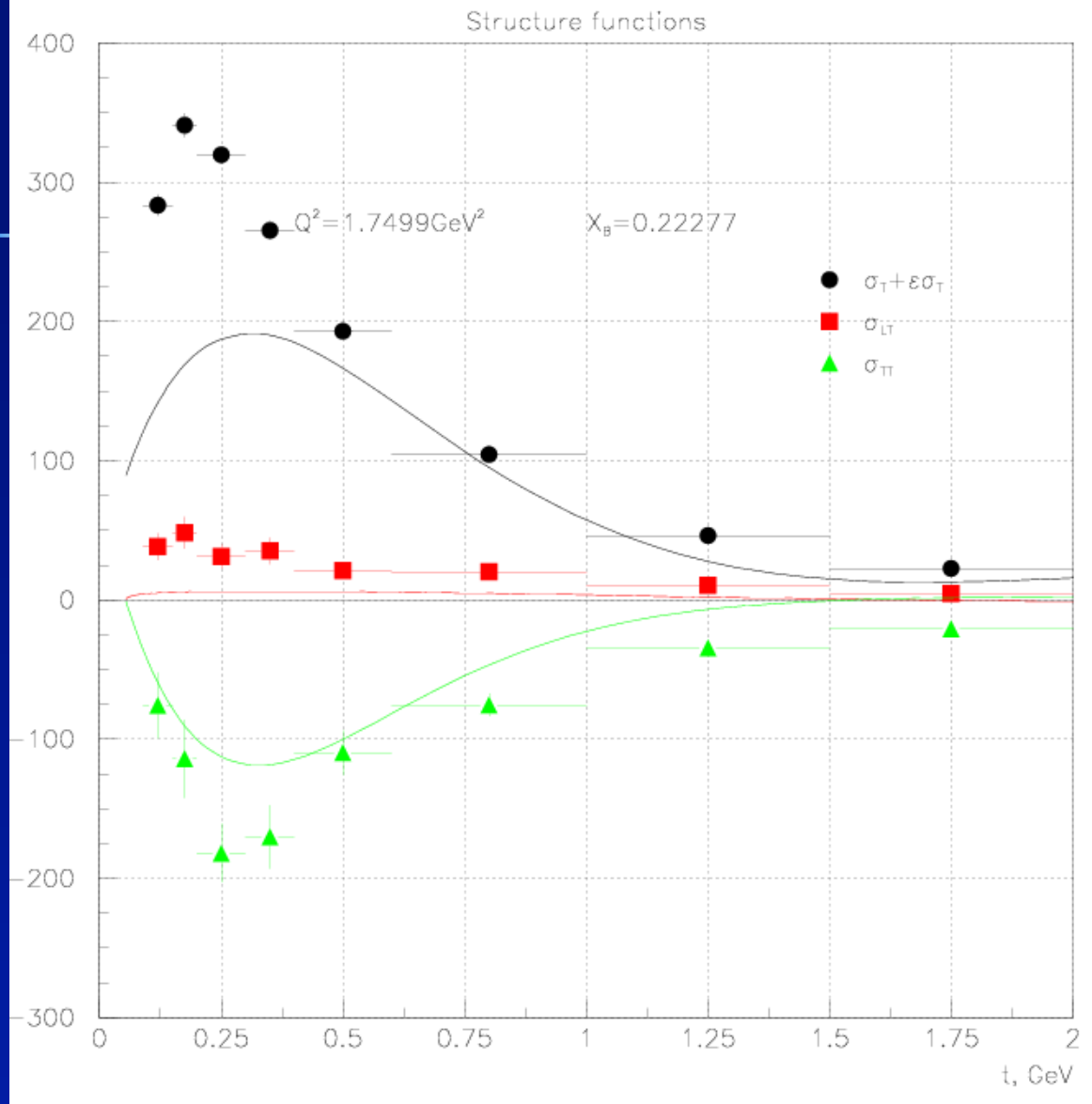
$Q^2 = 1.15 \text{ GeV}^2$
 $X_B = 0.13$



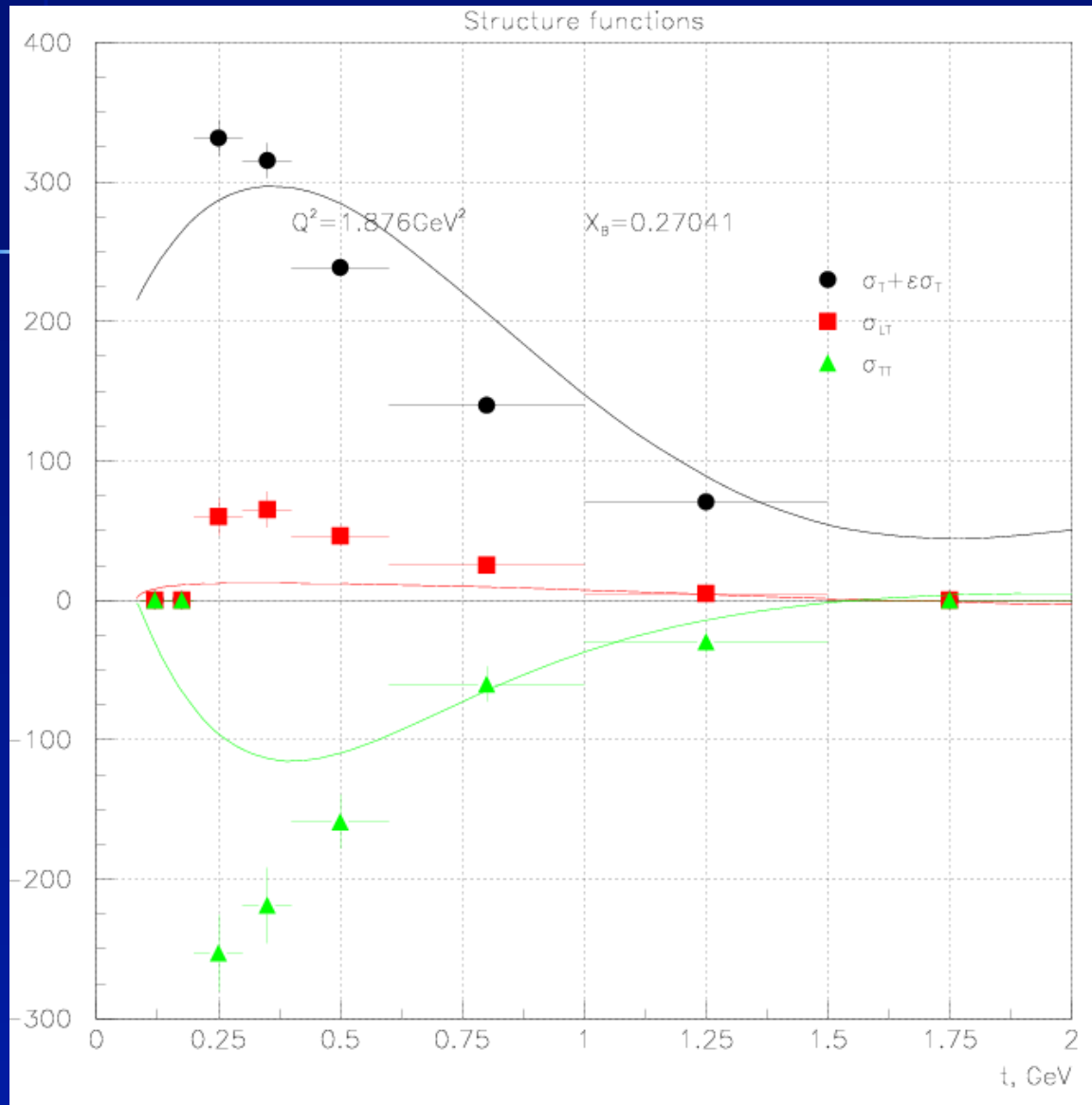
$Q^2 = 1.38 \text{ GeV}^2$
 $X_B = 0.17$



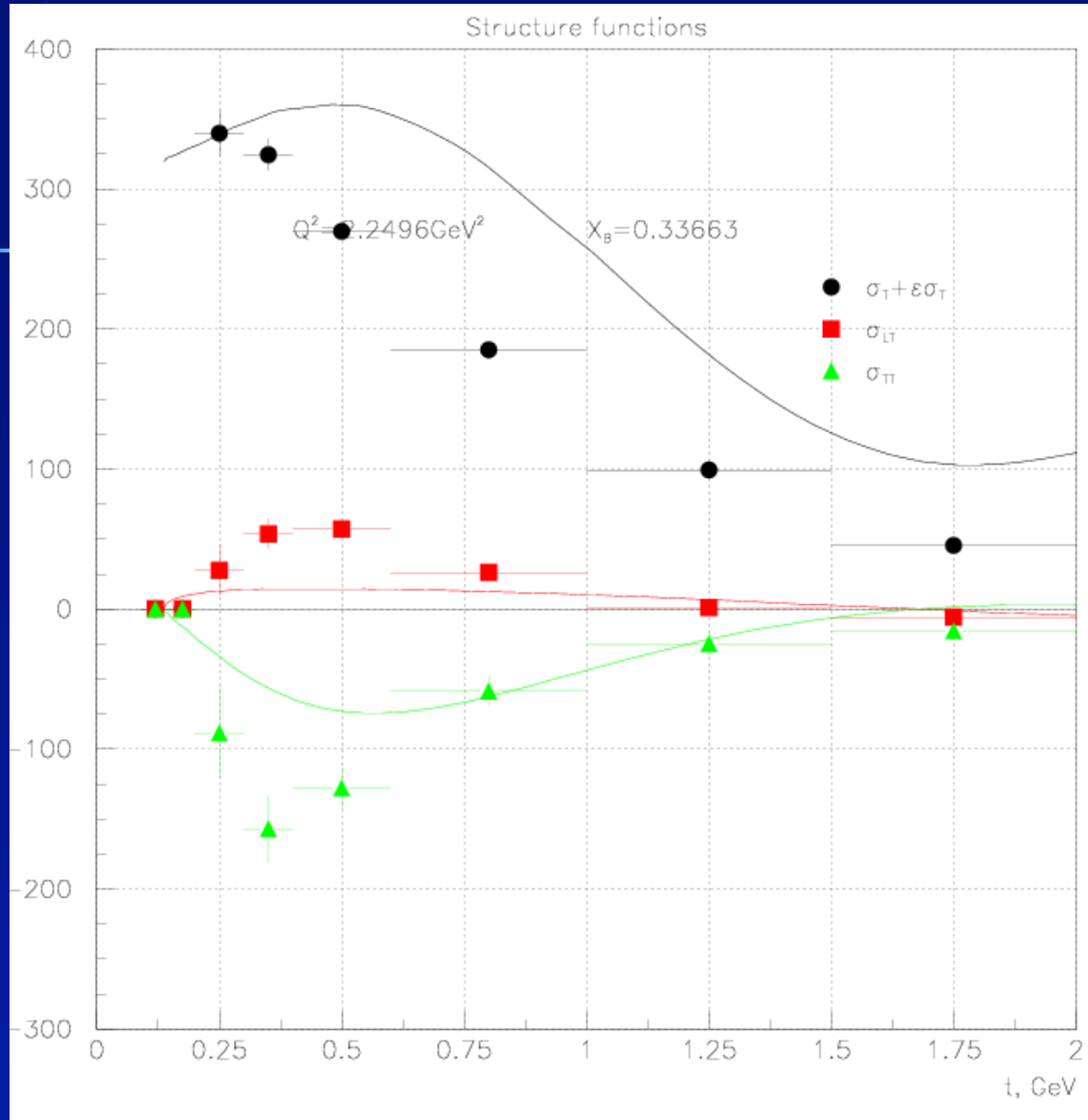
$Q^2 = 1.61 \text{ GeV}^2$
 $X_B = 0.19$



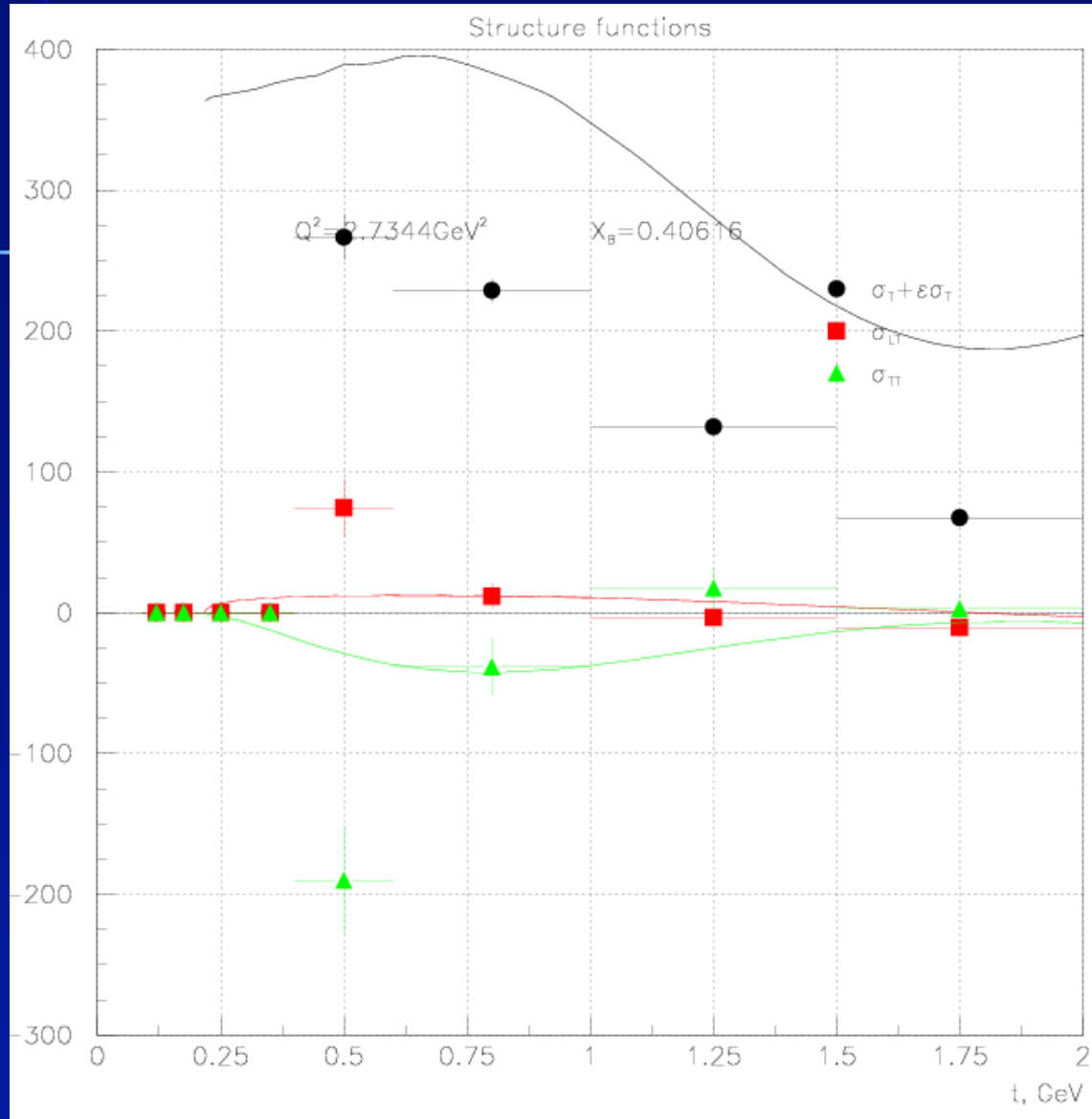
$Q^2 = 1.74 \text{ GeV}^2$
 $x_B = 0.22$



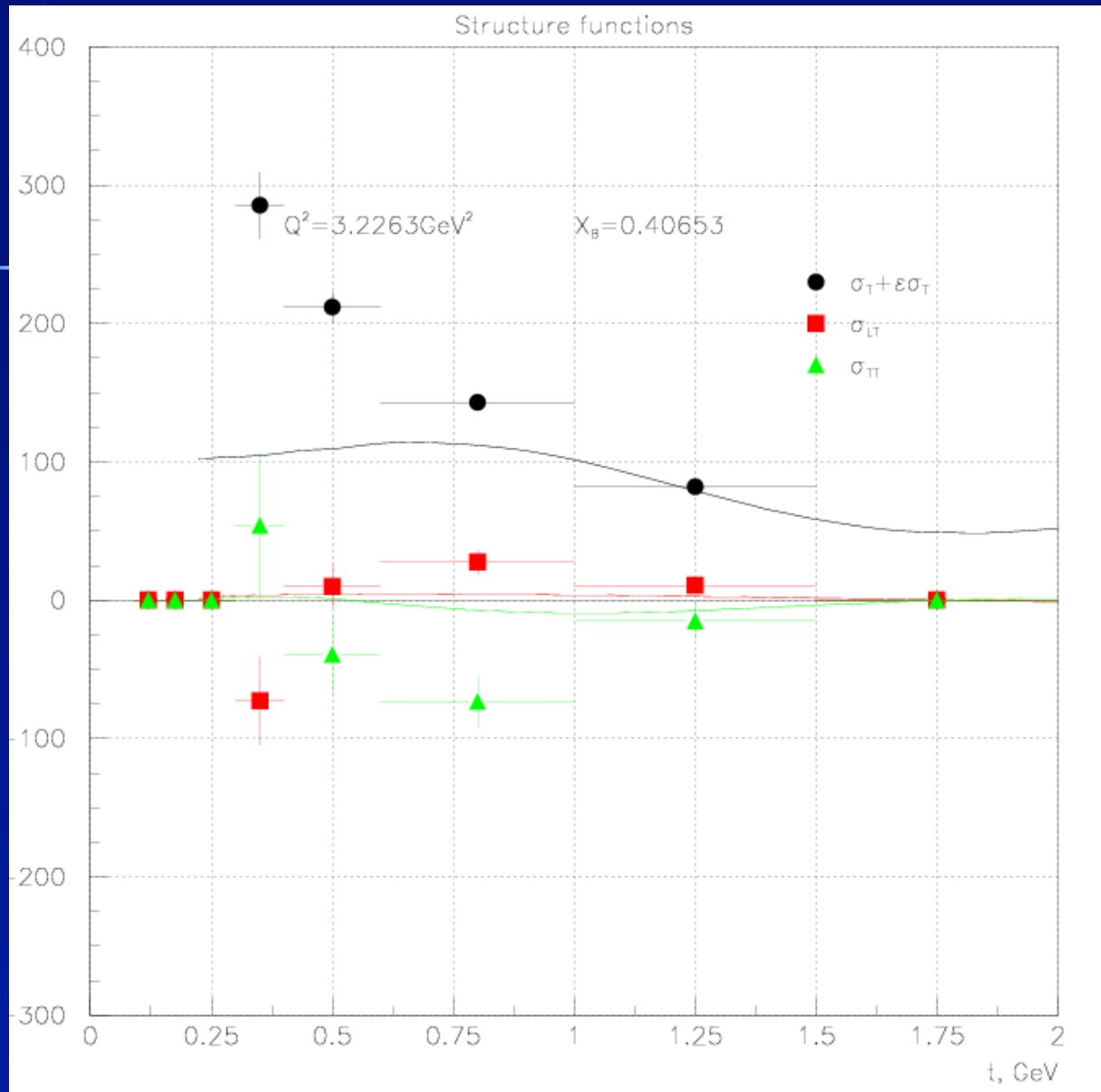
$Q^2 = 1.88 \text{ GeV}^2$
 $x_B = 0.27$



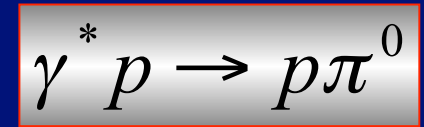
$Q^2 = 2.25 \text{ GeV}^2$
 $X_B = 0.34$



$Q^2 = 2.73 \text{ GeV}^2$
 $x_B = 0.41$

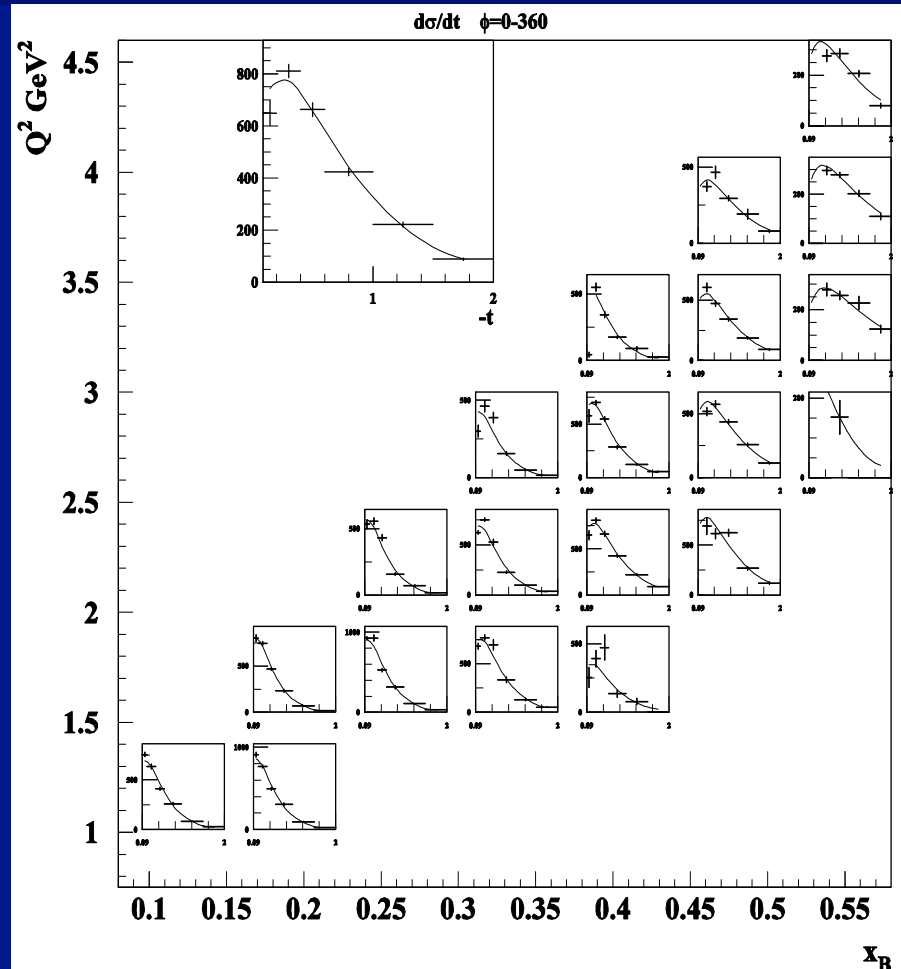


$Q^2 = 3.22 \text{ GeV}^2$
 $x_B = 0.41$



t - distribution

$$\frac{d\sigma}{dt} \propto e^{B(x_B, Q^2)t}$$



$$\gamma^* p \rightarrow p\pi^0$$

t-Slope Parameter as a Function of x_B and Q^2

$$\frac{d\sigma}{dt} \propto e^{B(x_B, Q^2)t}$$

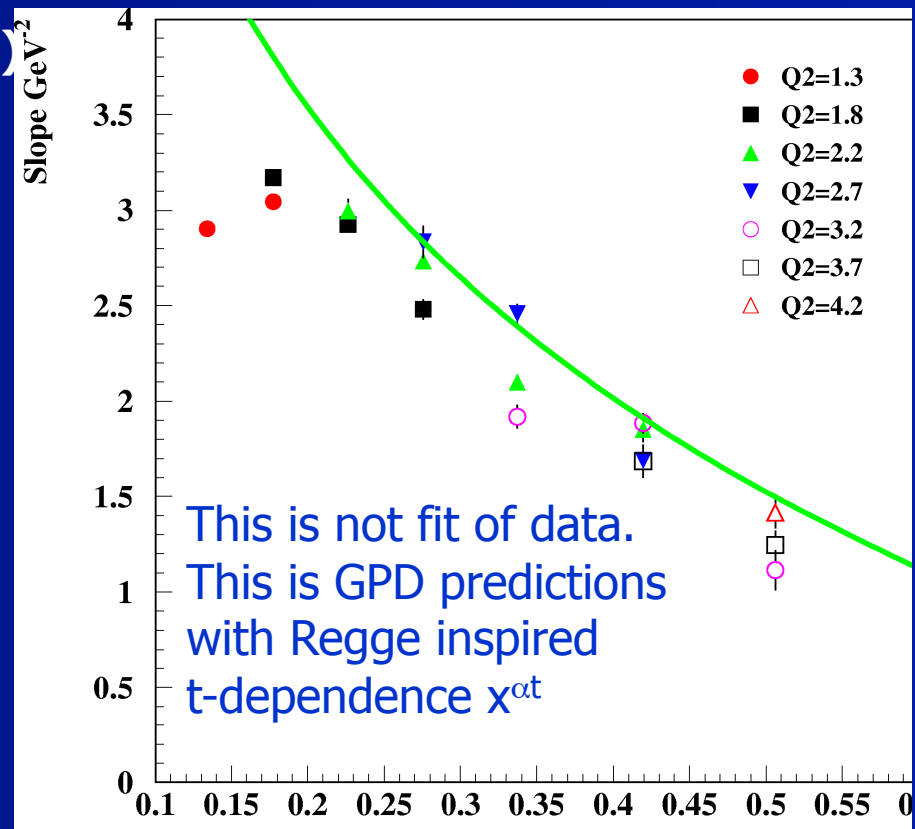
$$B(x_B, Q^2)$$

$$f^q(x, t) \propto x^{\alpha_q(t)} \propto x^{\alpha't}$$

$$\frac{d\sigma}{dt} \propto [x^{\alpha't}]^2 = e^{2\alpha'\ln(1/x)t}$$

$$B(x) = 2\alpha'\ln(1/x)$$

$$\alpha' = 1.1$$



• $B(x_B, Q^2)$ is almost independent of Q^2

• $B(x_B)$ is decreasing with increasing x_B

x_B

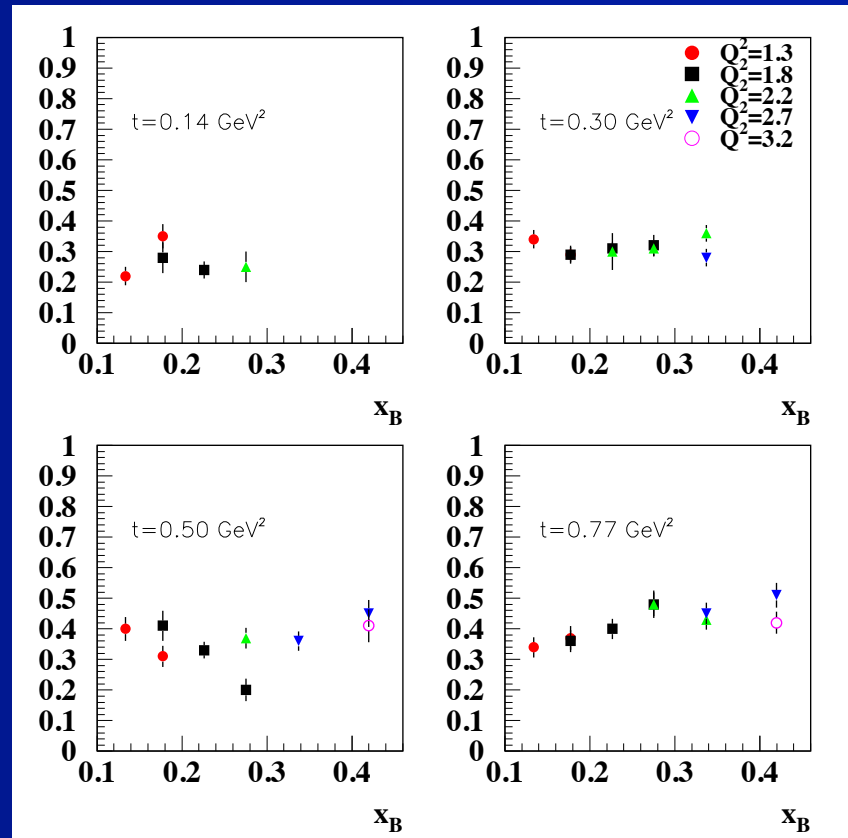
η/π^0 Ratio

$$\frac{\sigma(ep \rightarrow ep\eta)}{\sigma(ep \rightarrow ep\pi^0)}$$

Preliminary data on the ratio η/π^0 as a function of x_B for different bins in t .

The dependence on the x_B and Q^2 is very weak.

Probably we have small positive slope. The ratio in the photoproduction is near 0.2-0.3 (very close to what we have at our smallest Q^2).



π^0 and η Beam Spin Asymmetry

$$\frac{d\sigma}{dtd\phi}(Q^2, x, t, \phi) = \frac{1}{2\pi} \left(\frac{d\sigma_T}{dt} + \varepsilon \frac{d\sigma_L}{dt} + \varepsilon \frac{d\sigma_{TT}}{dt} \cos 2\phi + \sqrt{2\varepsilon(\varepsilon+1)} \frac{d\sigma_{LT}}{dt} \cos \phi \right. \\ \left. + h\sqrt{2\varepsilon(\varepsilon-1)} \sin \phi \frac{d\sigma_{L'T}}{dt} \right)$$

h is the beam helicity

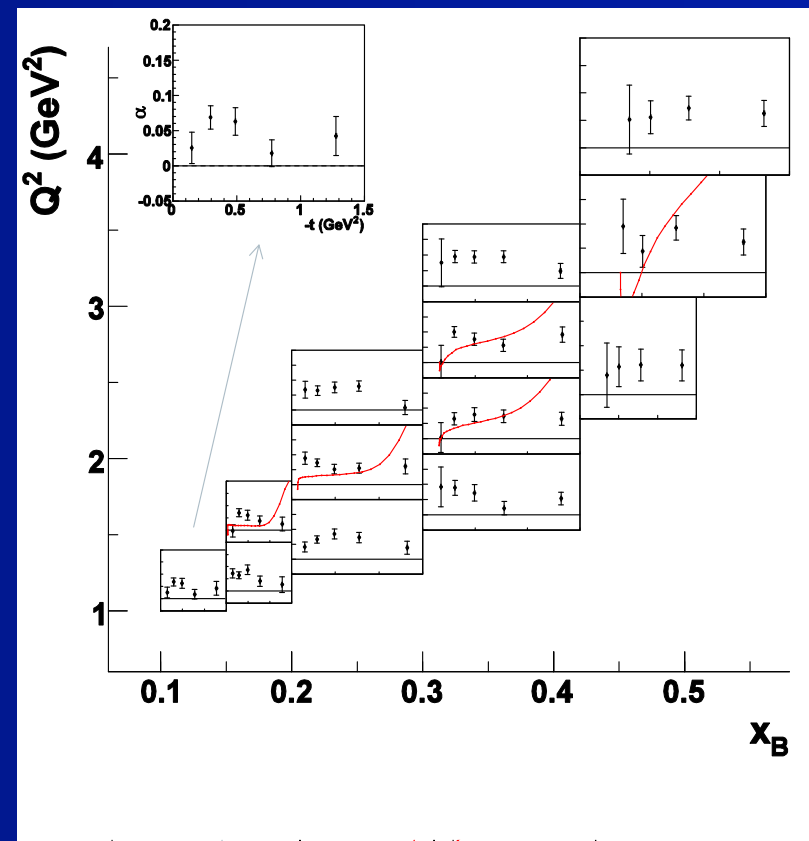
$$A = \frac{d^4 \vec{\sigma} - d^4 \bar{\sigma}}{d^4 \vec{\sigma} + d^4 \bar{\sigma}} \approx \alpha \sin \varphi$$

Any observation of a non-zero BSA would be indicative of an L'T interference.
If σ_L dominates, σ_{LT} , σ_{TT} , and $\sigma_{L'T}$ go to zero

$$\gamma^* p \rightarrow p\pi^0$$

Beam Spin Asymmetry

- The red curves correspond to the Regge model (JML)
- BSA are systematically of the order of 0.03-0.09 over wide kinematical range in x_B and Q^2

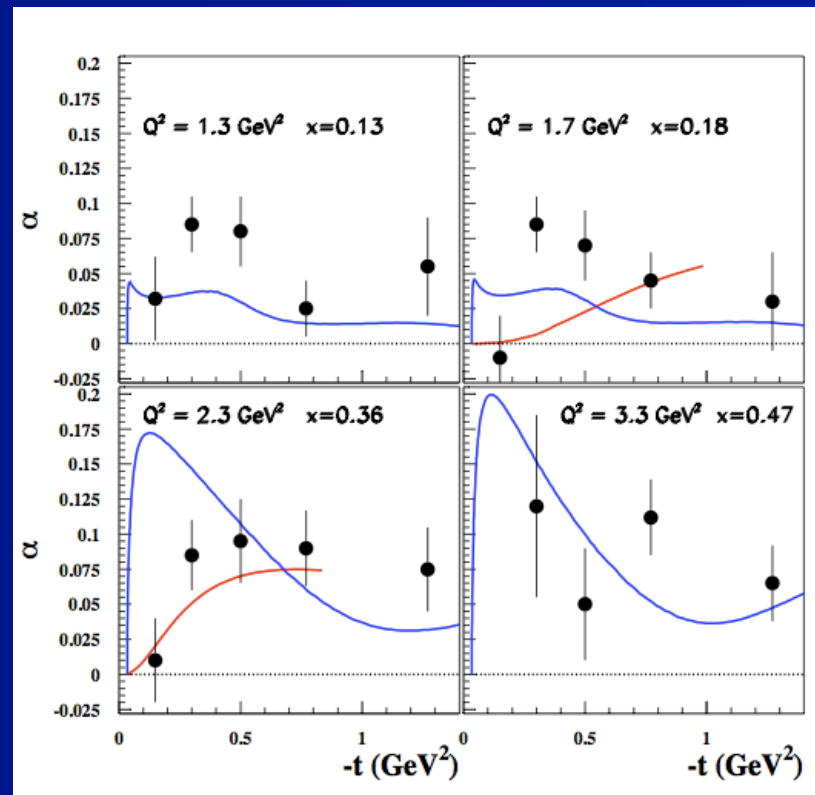


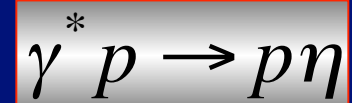
$$\gamma^* p \rightarrow p\pi^0$$

Beam Spin Asymmetry

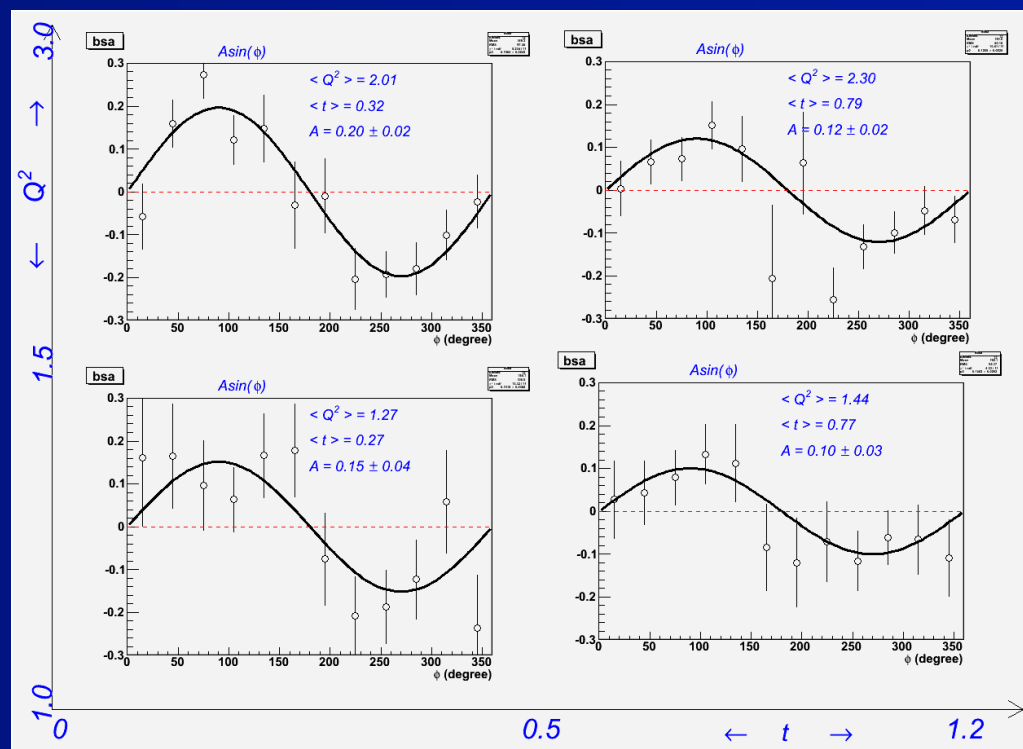
Ahmad, Goldstein, Luiti, 2009

- Data CLAS
- Blue – Regge model
- Red – GPD predictions
- tensor charges
 - $\delta u = 0.48,$
 - $\delta d = -0.62$
- transverse anomalous magnetic moments
 - $\kappa^u_T = 0.6,$
 - $\kappa^d_T = 0.3.$

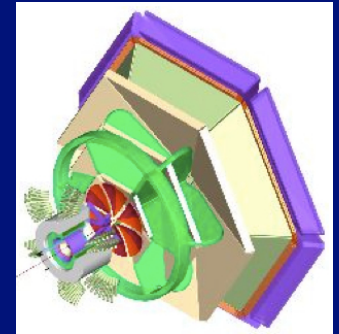




η Beam Spin Asymmetry

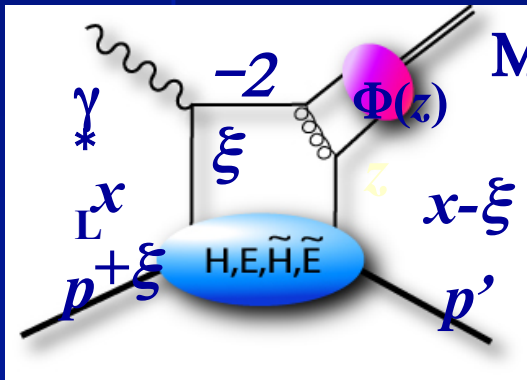


Summary



- Deeply Virtual Meson Production has the potential to probe the nucleon structure at the parton level, as described by Generalized Parton distributions (GPDs).
- The most extensive set of π^0 and η electroproduction data to date has been obtained with the CLAS spectrometer.
- Structure functions, the π^0/η ratio of the cross sections and beam-spin asymmetries were extracted in the valence quark region.
- Sizable interference terms σ_{TT} and σ_{LT} and non-zero asymmetries imply that both transverse and longitudinal amplitudes participate in the process.
- The detailed comparison with the Regge model predictions was done. The model describes the data reasonably well.
- We are working with theorists who are doing the calculation of the DVMP cross sections within the handbag GPD based models. The comparison results are coming.
- CLAS12 will continue the GPD study with broader kinematics at 12 GeV machine.

The End



+

